THE UNIVERSITY
OF QUEENSLAND
AUSTRALIA

`

THE UNIVERSITY OF QUEENSLAND

Bachelor of Engineering Thesis

Environmental-friendly Thermoelectric Materials

Student Name: Christine AUSTIN

Course Code: MECH4500

Supervisor: Dr. Chen Zhigang

Submission Date: 28 October 2016

A thesis submitted in partial fulfilment of the requirements of the Bachelor of Engineering degree in
specialization of Mechanical and Materials Engineering

Abstract

Since decades ago, thermoelectric materials have been recognized as a potential energy conversion technology due to its ability to convert heat into electricity directly. Despite that, the low efficiency and the complexity in fabrications of thermoelectric devices restrict their applications commercially. Other than that, some thermoelectric materials such as lead telluride or bismuth telluride pose threat to the environments due to their toxicity in their substance. While the current research to obtain an environmental friendly and yet abundance thermoelectric materials to be used in large quantities are currently scarce and less interested due to the lower efficiency of the materials. In this final report, I will do a complete literature review and summarize environmental friendly thermoelectric material (silicide- based). First of all, I will introduce the basic principles of thermoelectric materials, and then followed by discussing several methods to improve the ZT value of thermoelectric materials. After that a detailed overall summary of types of silicon-based thermoelectric materials will be elaborated. Finally, conclusion and future progresses in accordance to the review will be specified.

Upon reviewing the research papers, it was found that:

- Current highest achievement of ZT is 3 at 550 K by PbTe quantum superlattices.
- In terms of silicide based, highest experimental achievement of ZT is by double doping n-type $Mg_2Si_{0.75}Sn_{0.25}$ with Al and Sb at 850 K. Peak ZT of 1.4 is achieved from significant enhancement of the carrier concentration.
- Magnesium silicide, HMS and SiGe have been proven to achieve reasonable dimensionless figure of merit by doping and nanostructuring.
- Other types of silicides such as $FeSi_2$, $CrSi_2$, $ReSi_{1.75}$, CoSi and Ru_2Si_3 are included as potential thermoelectric materials for future industrial applications. However, not much experimental results are available in current research paper as the most results are obtained are calculated theoretically.
- Future recommendation is to analyse other types of thermoelectric material such as metal oxides and organic TE materials.

In general, this thesis report consists of a concise justification and description on the silicide-based environmental friendly thermoelectric materials.

Acknowledgement

First of all, I would like to express my special appreciation and thanks to my supervisor Dr. Zhigang Chen for his mentoring and guidance. Without his assistance and dedicated involvement in every step throughout the thesis process, this paper will have never been successfully accomplished. I would like to thank you for the kind support and understanding over this whole year of thesis.

I would like to express my gratitude to Professor Zhou Jin and the PHD team for allowing me to the weekly thesis discussion to improve my knowledge and understanding regarding my thesis topic.

Next, I would like to express my thank you to professor David Mee for the thesis seminar and guidance for the entire year of my thesis.

Most importantly, none of this could have happened without the support of my family and close friends. My parents, who offered me their encouragement through phone calls and texts every day. My brother, who motivated and inspired me not to give up during the hard times. At the end I would like to express my appreciation to my fellow mates for their advice and company during those sleepless nights when we were working together before the deadlines.

Table of Contents

List of Figures

List of Tables

Chapter 1: Introduction

In today worlds, constant increasing of energy demands, sudden climate change and depletion of fossil fuel resources has driven the demand for obtaining more sustainable technologies for efficiency use, conversion and recovery of energy. The global demands of fossil fuels and oil are continuously increasing over the years [21], while there are lack of renewable energy in the market and current available renewable energy such as combustion/gasoline engine has low efficiency. In fact, current modern gasoline engines have only 25-30% maximum thermal efficiency used to power a vehicle while 70-75% is rejected as waste heat [22]. Approximately half of the rejected heat is carried away by exhaust gases and another half passes through cylinder walls into engines cooling system and is lost to the atmosphere by radiation, friction, noise and air turbulence [23]. Furthermore, according to US Department of Energy [24], the waste energy assessment on United States indicated that more than 2/3 of fossil fuel (~64%) used to generate power and electricity is wasted as heat to the atmosphere. Other environment assessment by European environment Agency (EEA) stated that emissions from electrical power plant such as carbon dioxide, carbon monoxide, sulphur and methane poses high environmental problems resulting in pollution and global warming [25]. Therefore, the development of technologies for waste to heat recovery systems has high potential in future industry of power generation and cooling systems.

Thermoelectric materials with low cost (silicides, oxides or skutterudites) and high chemical stability (silicides and oxides) exhibit promising potential for current commercial applications where low price and high durability are an important consideration. Other advanced nanomaterials such as nanowires, nanocomposites or superlattices have increased the possibility of attaining better performance for optimization of thermoelectric generators [26].

The conversion efficiency of thermoelectric materials is strongly related to figure of merit (ZT) of the thermoelectric material. ZT is given by Eq. (1) as follows [27]:

$$ZT = \frac{S^2 \sigma T}{k} = \frac{S^2 T}{k \rho} = \frac{S^2 T}{(k_e + k_l) \rho} \tag{1}$$

Where S is the Seebeck coefficient, σ is the electrical conductivity, k is thermal conductivity, T is the absolute temperature, ρ is electrical resistivity. Seebeck coefficient (known as thermopower) is a metric that evaluates the ability of TE materials to convert heat into electricity directly. It has a unit of volts per kelvin (V/K). however, in most cases microvolts

per kelvin (μ V/K) are used. Seebeck coefficient often depends on structural, chemical and thermodynamic properties such as molecular structure, carrier concentration and effective mass [28].

Electrical conductivity is a measure of how good a material can accommodate to the movement of electrical charge. The SI unit of electrical conductivity is Siemens per meter (S/m). The values of electrical conductivity are affected by chemical composition or the state of crystalline structure [29].

Thermal conductivity is denoted as the capability of transferring heat through a material. As shown in equation 1, in order to achieve high ZT, low thermal conductivity is required. Thermal conductivity k consists of two parts: electric thermal conductivity k_e and lattice thermal conductivity k_l. Due to that, decreasing of thermal conductivity will lower the electrical conductivity too. One way to overcome this is using phonon scattering process [28].

In order for the efficiency of power generation and cooling system to be high, the ZT value of thermoelectric materials must be enhanced to a certain level. As a consequence, thermoelectric research and experiment have been focussed on the optimization of improving the figure of merit. In order to maximize ZT, which in turn maximizing the efficiency of a material, both σ and S are required to be large while k must be minimized [30].
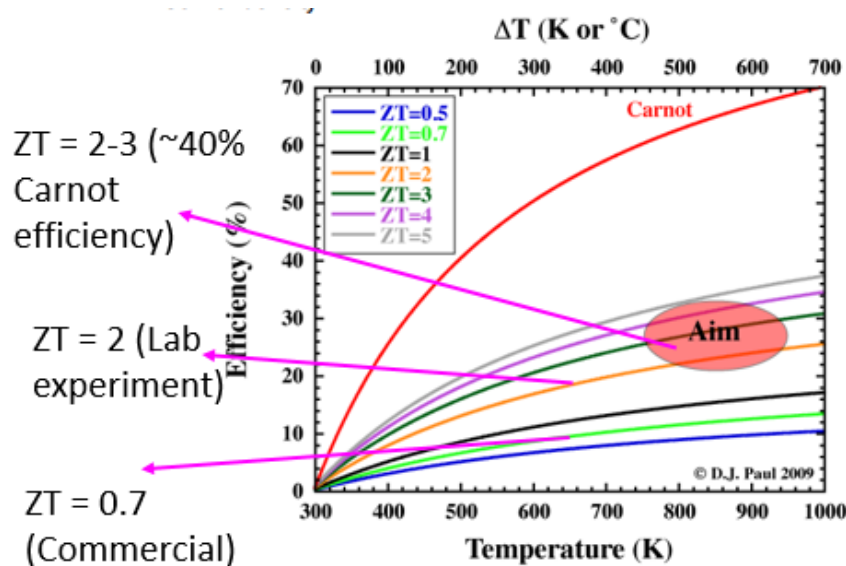
Figure 1: Thermoelectric energy conversion as a function of ZT, assuming the cold side temperature = 300 K.

Fig. 1 shows the dependence of conversion efficiency of ZT. It can be seen that in order for thermoelectric materials to be in the same competence as conventional heat engines hence applicable in commercial use, ZT of TE materials much be > 3 (~40% of Carnot efficiency).

Several significant progresses in improving the thermoelectric properties are shown in fig. 2, which includes major milestones achieved for ZT over several decades as a function of year.
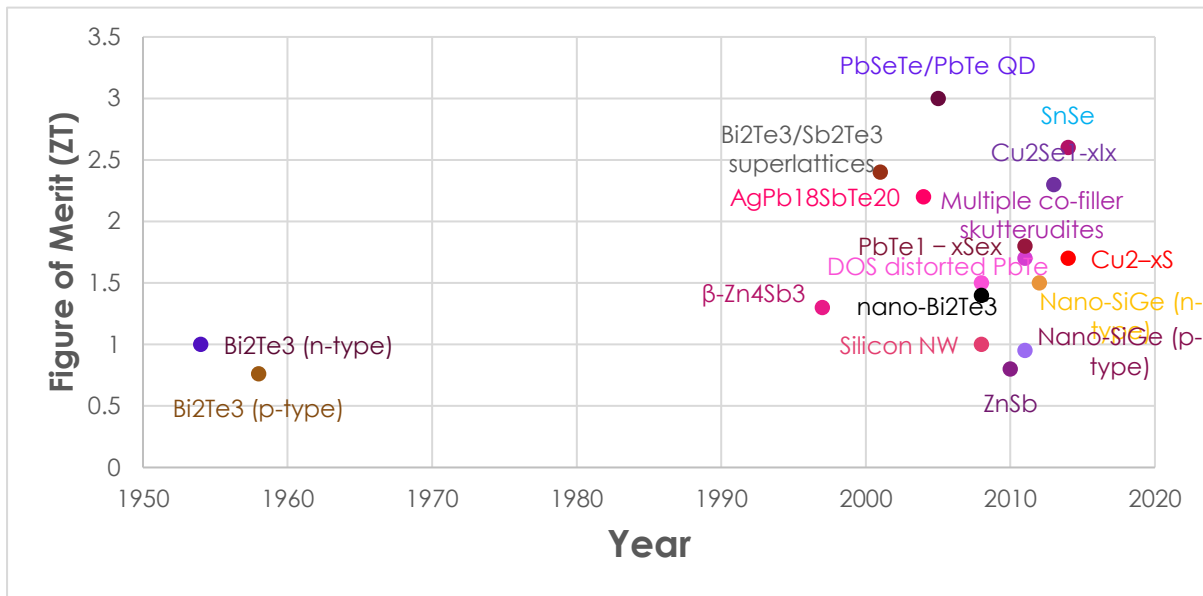
Figure 2: ZT of current bulk thermoelectric material as a function of year indicating significant development of thermoelectric materials. Highest achievement of ZT = 3 is achieved by quantum-dots Bi-doped n-type PbSeTe/PbTe at 550 K [31]. Bi_2Te_3 [32]; Bi_2Te_3 [33]; β-Zn_4Sb_3 [34]; Bi_2Te_3/Sb_2Te_3 super lattices [35]; $AgPb_{18}SbTe_{20}$ [36]; DOS distortion PbTe [37]; p-type nano-Bi_2Te_3 [38]; Silicon NW [39]; Single phase ZnSb [40]; Nano-SiGe (p-type) [41]; Nano-SiGe (n-type) [42]; $PbTe_{1-x}Se_x$ [43]; multiple co-fillers Skutterudites $CoSb_3$ [44]; $Cu_2Se_{1-x}I_x$ [45]; SnSe [46]; $Cu_{2-x}S$ [47]. Currently, no material has yet to achieve ZT > 3.

Fig. 2 summarizes achievement of ZT values over past several decades as a function of year. There was not much improvement on the research on the TE material from 1960s to 1990s. The research of thermoelectric materials has finally found a turning point when Hicks and Dresselhaus [48] verified that the improvement of ZT in two dimensional Bi_2Te_3 is possible due to the quantum confinement effects. They also proved that ZT of a highly anisotropic material can be increased significantly by layering the super lattice to scatter phonons resulting in the decrease of thermal conductivity. Currently, the highest achievement of ZT (ZT = 3 at 550 K) was reported by Harman et al. [31] in 2005 by doping n-type PbSeTe/PbTe quantum dot superlattice (QDSL) doped with bismuth.

Nanostructured thermoelectric materials have been a significant research subject since few decades ago. Several good reviews have been conducted including bulk nanostructured thermoelectric materials [27, 49], bulk materials [50] and environmental friendly TE materials such as oxide-based [2, 51], organic based [52-55], silicide-based [56, 57] and etc. Although there existed several good reviews on single environmental friendly TE material, there were not much overall review on the whole environmental material itself. Hence, I will do a detailed review on environmental friendly thermoelectric materials and highlighted significant progress of environmental friendly TE material in the past several decades. The organization of the review is as follows. Firstly, I will discuss on the fundamental methodology to improve the performance of thermoelectric material. Next, I will focus on addressing and summarizing silicon-based thermoelectric materials including magnesium silicides, high manganese silicides, silicon germanium, iron disilicides, chromium disilicide, cobalt monosilide, rhenium silicide and ruthenium silicide. Finally, conclusion and future progress will be justified.

Chapter 2: Literature Review

2.1 Methodology for improving figure of merit (ZT)

Equation (1) demonstrates that material with high ZT can be achieved by improving the Seebeck coefficient and electrical conductivity, while maintaining thermal conductivity as low as possible. Electrical conductivity σ of TE materials can be expressed as follows:

$$\sigma = \frac{1}{\rho} = ne\mu \qquad\qquad (2)$$

Where n is the carrier concentration, e is the charge of unit carrier and μ is the carrier mobility. Electrical conductivity can be enhanced through addition of chemical dopants. Doping will decrease the charge carrier's mobility due to the increased of scattering between the dopants and carriers. In addition, each dopant's atom has one more/less valence electron compared to the host atoms therefore can increase the density of charge carriers [3]. According to Powell and Vaqueiro [4], good thermoelectric material usually is heavily doped narrow bandgap semiconductor with charge carrier densities in the range of 10^{19} to 10^{21} cm^3 as shown in Fig. 3(a).

In order to ensure large Seebeck coefficient, only a single type of carrier (either n-type or p-type) is remained. Mixed n-type or p-type carriers will affect both of the carrier to remain at

the cold sides resulting in the opposite of Seebeck effect hence low thermopower. Large Seebeck coefficient can be existed in low carrier concentration insulators/semi-conductors with electrical conductivity as a trade-off. While high carrier concentration metals have high electrical conductivity but sacrificing their Seebeck coefficient [3]. The comparison of thermoelectric properties of metals, semiconductors and insulators at room temperature is shown in table 1. Though metals have good electrical conductivity, but their low Seebeck coefficient and large thermal conductivity decreasing the TE properties of metals. Insulator with large bandgaps have high Seebeck coefficient but extremely low electrical conductivity resulting in low power factor and small ZT. Therefore, optimum value of power factor is located between the carrier concentrations of metals and semi-conductor as shown in fig. 3(b).

TE property	Metals	Semi-conductor	Insulator
Seebeck Coefficient	$\sim$ 200-300 µV/K [58]	$\sim$ 0-3 µV/K [58]	$\sim$ 1000 µV/K [59]
Electrical conductivity	> 10^5 (s.m)$^{-1}$ [60]	$10^{-6} < \sigma < 10^5$ (Ω.m)$^{-1}$ [60]	< 10^{-6} (Ω.m)$^{-1}$ [60]
Carrier concentration	High	Low	Low

Table 1: Comparison of thermoelectric properties of metals, semi-metals and non-metals at 300K

The relationship between Seebeck coefficient and carrier concentration can be expressed in equation (8) as follows:

$$S = \frac{8\pi^2 K_B{}^2}{3eh^2} m^* T \left(\frac{\pi}{3n}\right)^{\frac{2}{3}}$$

(3)

Where m* is effective mass of the charge carrier, K_B and h are Boltzmann constant and Planck constant, respectively.

In order to achieve high ZT value, an effective TE material required to have low thermal conductivity. Thermal conductivity can be decreased by increasing the phonon scattering between the phonon-boundary, phonon-defects and phonon-phonon. Thermal conductivity of TE material consists of electron thermal conductivity (k_e) arising from the heat carrying charge carriers travelling through crystal lattice and lattice thermal conductivity (k_L) resulting from

heat transporting phonon travelling through the crystal lattice [49, 61]. The relationship between k_e and k_L is shown as follows:

$$k_{tot} = k_e + k_L \qquad (4)$$

Electron thermal conductivity is related to Weidemann-Franz Law [62] as shown in equation (10) below:

$$k_e = L\sigma T \qquad (5)$$

Where L is Lorenz number. Figure 3(b) shows that electrical thermal conductivity k_e is proportional to electrical conductivity hence reducing k_e is not always a reliable choice as it will affect the electrical conductivity resulting in minor or no improvement of figure of merits. Therefore, in semiconductors of thermoelectric materials, usually >90% of total thermal conductivity is originated from lattice thermal conductivity (k_L), hence reducing lattice thermal conductivity will lead in improvement of the thermoelectric properties [49, 61].
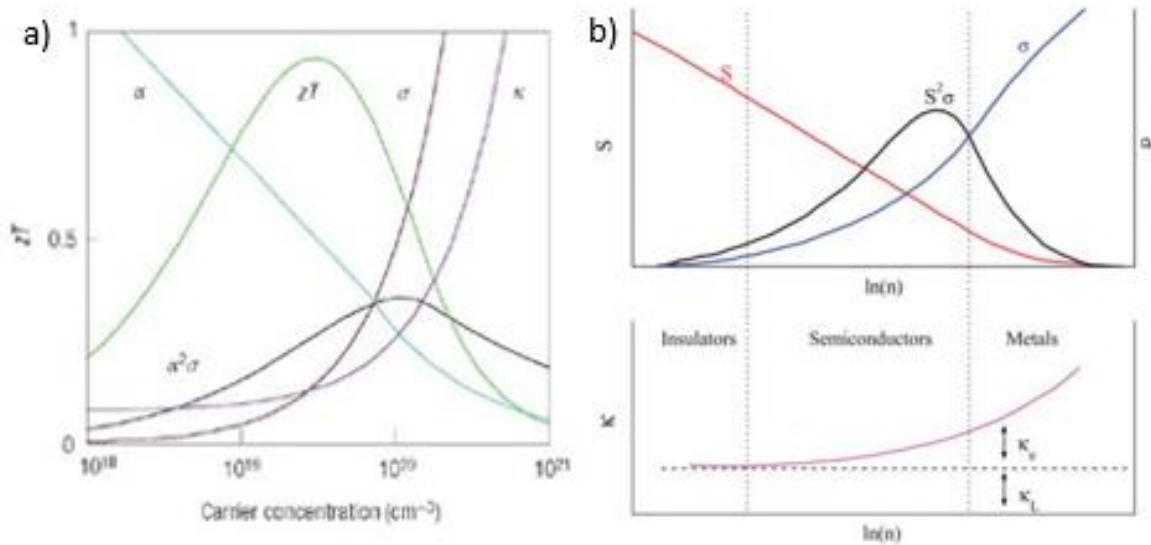
Figure 3: Maximizing efficiency (ZT) of TE involves compromising thermal conductivity (k) and Seebeck coefficient (S) with electrical conductivity (σ). Good thermoelectric materials are typically heavily doped semi-conductors with a carrier concentration between 10^{19} and 10^{21} carriers per cm^3. Thermoelectric power factor ($S^2\sigma$) maximizes at higher carrier concentration than ZT. Trends shown were modelled from Bi_2Te_3. Reproduced from Ref.[3]; (b) Illustration of variation of Seebeck coefficient (S), electrical conductivity (σ), power factor ($S^2\sigma$), electronic thermal conductivity (k_e), and lattice thermal conductivity (k_L) on the charge carrier concentration n, for bulk material. Reproduced from Ref.[4].

2.2   Recent progress in environmental friendly TE materials

As illustrated in figure 2, the development of thermoelectric materials is becoming more established since 1950. Although there are many types of TE materials that were found to achieve high ZT such as PbTe [31, 37, 50, 63, 64], Bi_2Te_3[35], and PGEC thermoelectric materials [49], most-state-of-the-art high-performance TE materials are toxic, harmful, expensive and non-environmental friendly. Fig. 4a shows the periodic table of various elements in terms of metal compositions. Circled elements indicated they are highly toxic and not suitable to be used in this category. Elements highlighted in red, yellow and green are considered as heavy metal, and hence they are toxic and their usage must be controlled and monitored. Other elements have minor negative or non-negative impacts on environment depending on their amounts [65]. Fig. 4b shows various thermoelectric materials for waste heat harvest and refrigeration applications in terms of temperature range of operations. According to He, Liu et al [2], silicides and oxides are considered as eco-friendly thermoelectric materials due to its low contaminants and abundance
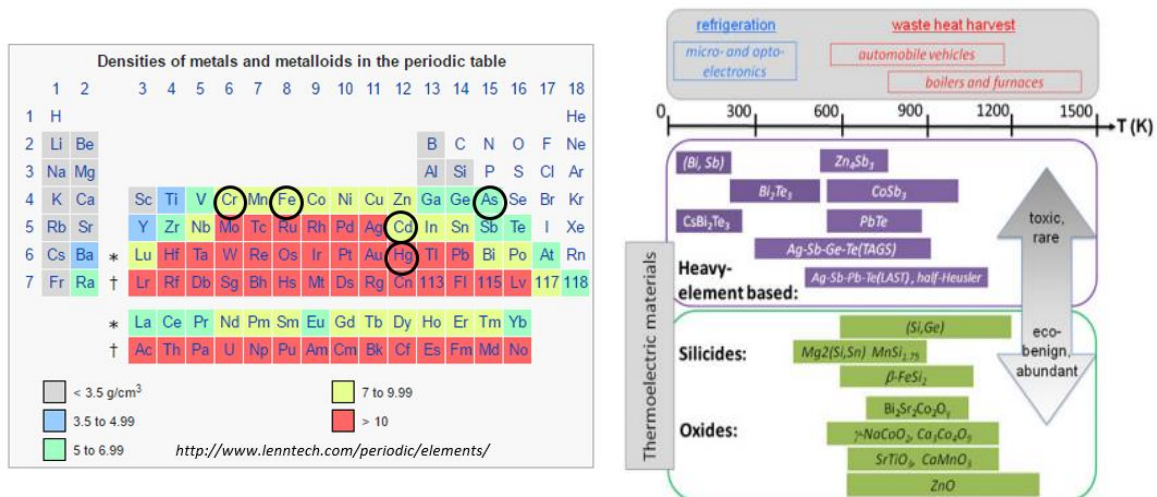
Fig.4 (a) Densities of metal in each elements of periodic table. Reproduced from Ref. [1]; (b) Application temperature range of waste heat and cooling system for different types of TE materials. Reproduced from Ref [2].

level in the nature. Other materials such as SnTe (an alternatives TE material for replacing PbTe) and organic TE materials such as PEDOT, polyacetylene and polyaniline are considered in this category too. In this report, our scope is only up to silicon-based TE materials while others material specified above will not be included in the review.

2.2.1 Silicon-based TE materials

Silicon is one of the most common and widely used semiconductor in industrial processes due to its environmental friendly, low-cost and high abundance in earth crust [66, 67]. However, due to its high thermal conductivity (k_L = 140W/m K) at room temperature, bulk silicon is known as poor TE material with ZT = 0.01 at 300 K [68]. This drawback was overcome by reducing the grainsize using nanotechnology. Recently, Hochbaum et al [69] reported 100-fold decrease in lattice thermal conductivity in silicon nanowires resulting in ZT=0.6 at room temperature. According to Hochbaum et al [69] the reduction of lattice thermal conductivity (k_L) of nanostructured Si is due to the strong phonon scattering from the increase of surface and interfaces from nanotechnology.

In 2009, Bux, Blair et al [70] also reported a ZT of 0.7 at 1275 K for n-type nanostructured bulk Si by reducing its thermal conductivity from nanostructuring the silicon with limited degradation in its electron mobility. This result shows a 90% reduction in its k_L due to interfacial phonon scattering. Similarly as stated by Hochbaum et al, Yang et al [71] commented that in silicon nanocomposites the value of k_L is minimised by the increasing of phonon scattering while preserving electron transport resulting in higher ZT. Yang et al also reported that nanoporous Si with randomly distributed pores exhibits very low k_L (< 0.1 W/m K) at 300 K, ~ three orders of magnitude lower than the bulk counterpart, leading nanoporous Si has a bright prospect in thermoelectric applications.

Yang and Li [41] in 2011 used nanothermodynamics model to calculate lattice thermal conductivity of nanoporous, nanocrystalline and nanostructured bulk Si. They found that 1) from boundary scattering and intrinsic size effect can significantly decrease lattice thermal conductivity by order of 1-2; 2) due to porosity effect, nanoporous Si exhibits smaller k_L compare to Si nanowires; 3) fully dense Si nanocomposites with finer grain size have comparable k_L with Si nanowires.

As stated above, silicon nanostructured materials exhibit promising future in TE applications due to its low cost, abundance, non-destructive to environment and the possess large effective mass and mobility to achieve high ZT hence they are deemed suitable for commercialised applications especially in semiconductor industry. Nielsch and Bachmann et al [72] considered silicon nanostructured as an emerging candidates for high efficiency and large volume production in the TE applications. In addition, the performances of Si nanostructures can be

further enhanced by doping with metals such as with germanium, manganese, chromium, iron and magnesium.

Crystal structure of silicon based thermoelectric materials are shown in table 2 below. The table show that magnesium silicide has cubic symmetry while other types of silicides have lower symmetries. Although most silicide possesses different crystal structure, most of these structures (expect for $CrSi_2$) are considered as deformed of a tetragonal structure. Hence, the possibility of finding anisotropy material properties are high.

Material	Syngony	a (nm)	b (nm)	c (nm)	a°	reference
Mg_2Si	Cubic	0.6338	-	-	-	[73]
$FeSi_2$	Orthorhombic	0.9863	0.7791	0.7833	-	[74]
$CrSi_2$	Hexagonal	0.4431	-	0.6364	-	[75]
Ru_2Si_3	Orthorhombic	1.1074	0.8957	0.5533	-	[76]
Mn_4Si_7	Tetragonal	0.5525	-	1.7463	-	[77]
$ReSi_{1.75}$	Monoclinic	0.3138	0.312	0.767	89.9	[19]

Table 2: Crystal structure of silicides thermoelectric materials.

2.2.1.1 Mg_2Si-based TE materials

Mg_2Si belongs to the family of magnesium (IV) compounds with that crystallises in antiflouride structure with FCC Si positions and tetrahedral Mg sites. Since 1960s, Mg_2Si-based thermoelectric materials have been regarded as potential thermoelectric material in the mid-temperature range from 500 to 900 K due to their high achievement in figure of merit ZT =1.3 [66, 78, 79]. Compared to other TE materials that have the same operating temperature range such as PbTe and $CoSb_3$, Mg_2Si are considered as a more attractive material for TE applications due to their low toxicity, thermal stability, relative abundance (Fig.5b shows the abundance of Mg and Si), higher resistance to oxygen and low production cost [61, 66, 80]. In addition, Mg_2Si is consisted of relatively light metals hence it has a low density (~1.99 g/m^3) which makes Mg_2Si a promising feature in the automobile heat recovery applications [8].
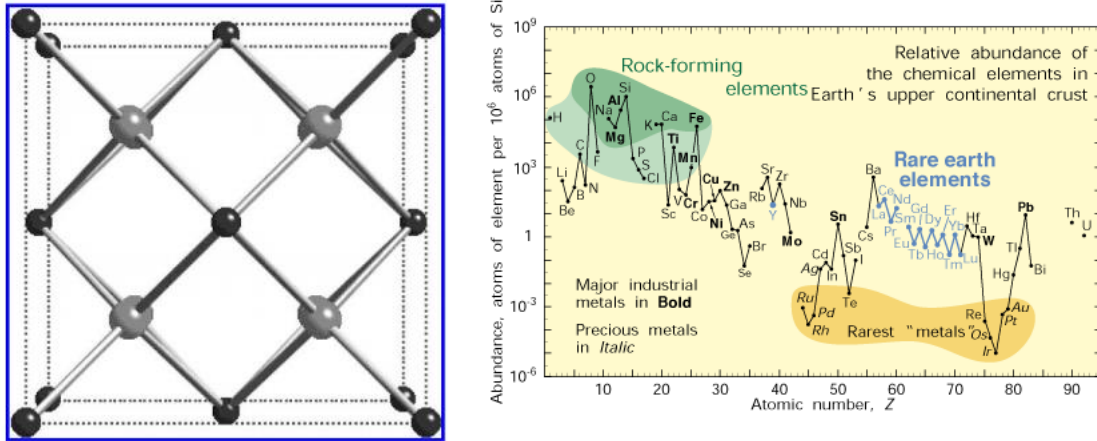
Figure 5: (a) Unit cell of Mg₂Si. It is a face centred (Fm3m) lattice, with Mg simple cubic lattice such that each Mg (larger grey circles) is coordinated by four Si atom in tetrahedron, while Si (smaller black circles) is surrounded by eight cubic atoms of Mg. Reproduced from Ref. [5]; (b) abundance elements in Earth's upper contiental crust as a function of atomic number. Both Mg and Si are highly abudance rock forming elements. Reproduced from Ref. [6].

Due to the extremely close of the boiling point of pure Mg (1363 K) and the melting point of Mg₂Si (1358 K), processing and handling of Mg₂Si is difficult [81]. This conditions restrict the use of arc melting method for synthesizing the compounds. Therefore, other methods such as ball-milling, spark plasma sintering (SPS), combustion methods, hydrogen synthesis and mechanochemical sintering were used to synthesized Mg₂Si. Another problem with Mg₂Si is the high vapour pressure and the high reactivity of Mg leading to poor control over stoichiometry which can lead to vacancies and defects that can affect the carrier concentration and mobility. However, this condition can be solved by mechanochemical method. In 2011, Bux et al [66] doped Mg₂Si with Bi and synthesized using mechanochemical process. They reported a peak ZT of 0.7 at 775 K when 0.15 at% of Bi is added into Mg₂Si. The enhancement in the ZT is due to the significant decrease in the lattice thermal conductivity from the point defect scattering.

The ease of volatilization and oxidation of Mg restricted obtaining of high quality Mg₂Si. Fusion methods were used but were unable to control the composition, structure and performance of Mg₂Si due to the oxidation and volatilization. Segregation due to the difference in melting points and specific gravities of Mg, with the presence of Si might increase the difficulty in controlling the composition and adjusting the relationship between the Mg₂Si structure. Hence, spark plasma sintering (SPS) is used in most study due to the extremely large diffusion velocity at low temperature hence the oxidation of Mg can be avoided [82]. Hu, Mayson and Barnett [7] used SPS method to synthesized Mg₂Si with Al as dopant at 750ºC.

18

They reported max ZT of 0.58 at 844 K for $Mg(AZ)_2Si$ due to the increased in power factor and electrical conductivity from the high carrier concentration and mobility from Al dopant. Figure 6 below shows the dimensionless figure of merit of Mg_2Si and $Mg(AZ)_2Si$ bulk samples, being prepared at 750 °C for 10 min.
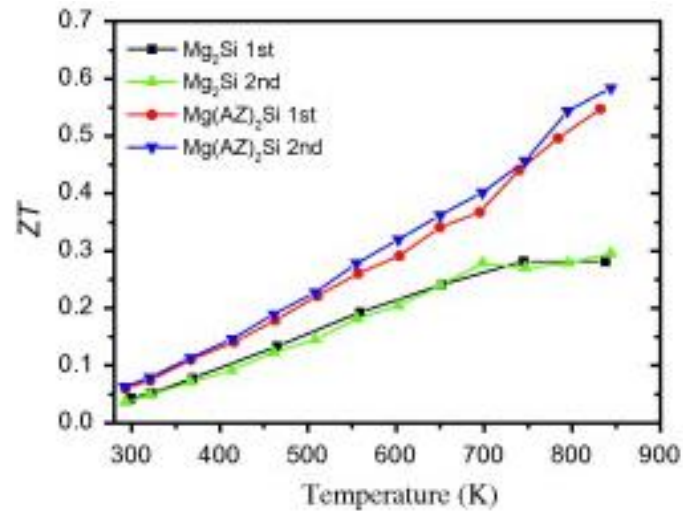
Figure 6: Dimensionless thermoelectric figure of merit, ZT for Mg_2Si and $Mg(AZ)_2Si$ bulk samples as a function of temperature. Reproduced from ref:[7]

Hu et al also commented that the possibility of higher electrical conductivity achieved in Mg_2Si is resulted from full densification of the material under SPS and low level of MgO. Using similar synthesis method, Tani and Kido [83] doped Mg_2Si with phosphorus and characterized by Hall effect measurements at room temperature for the electrical resistivity, Seebeck coefficient and thermal conductivity at (300-900K). From that, they calculated max ZT of 0.33 at 865K. Although Phosphorus (P) has the same Vb group as Sb and Bi hence it is considered as an attractive n-type dopant for Mg_2Si, the difficulty to fabricate due to the low melting point of P and high vapour pressure lowers the future research prospect for P-doped Mg_2Si. At the same year, similar processes has been done by the same research group [84] with Sb as dopant instead of P. Using same calculation technique and approaches, Tani and Kido reported a ZT of 0.56 at 862 K.

Undoped of Mg_2Si has narrow bandgap (~0.77eV) hence the ZT value of undoped Mg_2Si is very low (~0.1). The thermoelectric performance of Mg_2Si can be significantly enhanced when it is doped with proper dopants such as: for n-type dopants (Al, Sn and Bi); p-type dopants (Ag and Cu).

19

In 2010, Sakamoto et al [85] doped polycrystalline Mg_2Si with Al and Bi and achieved ZT of 0.77 at 862 K. At the same experiment, Sakamoto et al also doped Mg_2Si with 3 at % of Ag to achieved p-type Mg_2Si with lower achievement of ZT (0.11 at 873 K) compared to n-type Mg_2Si. The significant low Seebeck coefficient of Ag-doped Mg_2Si is the main reason for the low ZT obtained. In 2010, Isoda et al [86] investigated $Mg_2Si_{0.25}Sn_{0.75}$ doped with Li and Ag. Comparing the double doped samples with single doped samples, the double doped $Mg_2Si_{0.25}Sn_{0.75}$ has higher Seebeck coefficient compared to the single Li-doped Mg_2Si. Double doping also doubled the carrier concentration comparing to single doped. In 2014, Isoda et al [87] found highest ZT value of Al + Sb double doping of n-type $Mg_2Si_{0.75}Sn_{0.25}$ at 850 K using hot-pressing and liquid solid reaction synthesis. The carrier concentration is significantly enhanced by doping. Therefore, Sb is considered as effective dopants for increasing the carrier concentration in Mg_2Si.
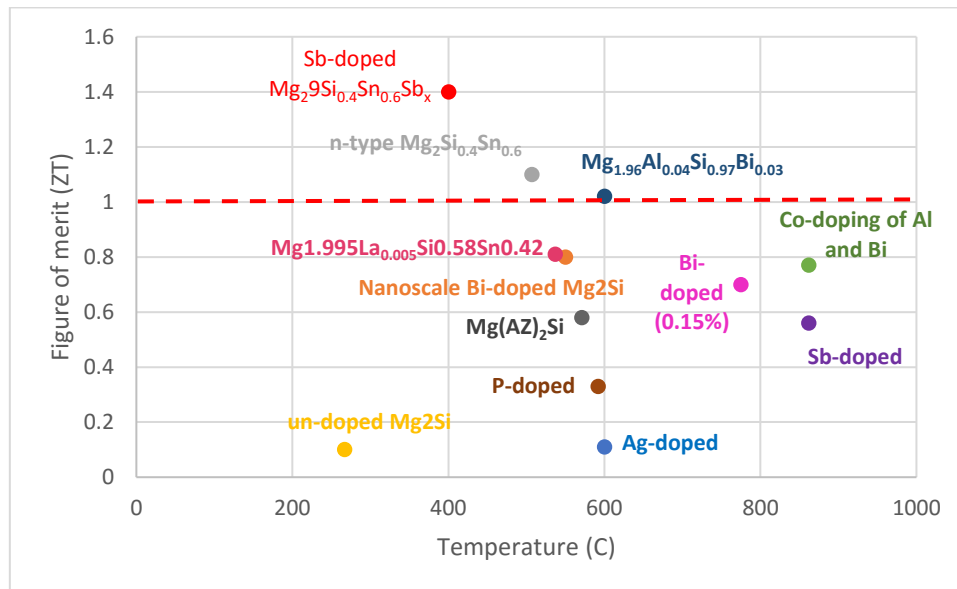
Figure 7: Maximum figure of merit values of p-type and n-type magnesium silicides with temperature range from 200 to 900°C. Highest achievement of ZT is by Sb-doping of $Mg_2Si_{0.4}Sn_{0.6}Sb_x$ solid solutions [80] while un-doped Mg_2Si achieved ZT of 0.1; other solid solution achieved ZT >1 are n-type $Mg_2Si_{0.4}Sn_{0.6}$ [88] and $Mg_{1.96}Al_{0.04}Si_{0.97}Bi_{0.03}$ [8] while ZT <1 is $Mg_{2-x}La_xSi_{0.58}Sn_{0.42}$ [89], Doping is added to enhance the ZT of Mg_2Si: Al- doping of $Mg(AZ)_2Si$ [7];phosphorus-doping [83]; Bi-doping [66]; Sb-doping [84]; Ag-doping [85]; and Al & Bi co-doping [85]. Nanostructure approach were conducted to improve the TE performances [71].

There are few ways to increase ZT of Mg_2Si: (1) Adding various elements as dopants such as Al, Sb, Bi and Na; (2) formation of homogenous solid solution of $Mg_2Si_{1-x}Ge_x$ and $Mg_2Si_{1-x}Sn_x$; (3) by nanostructuring [61]. Kim et al [8] co-doped polycrystalline Mg_2Si with Bi and Al via solid solution reaction and spark plasma sintering (SPS). They reported a maximum ZT of 1.02 is observed at 873 K in $Mg_{1.96}Al_{0.04}Si_{0.97}Bi_{0.03}$ due to the increase in power factor by

engineering density of states (DOS) and decrease in lattice thermal conductivity by point defect phonon scattering. Kim et al also found that addition of Al dopants on mg sites will increase the solubility limit of Bi on Si sites hence better thermoelectric performance can be achieved.
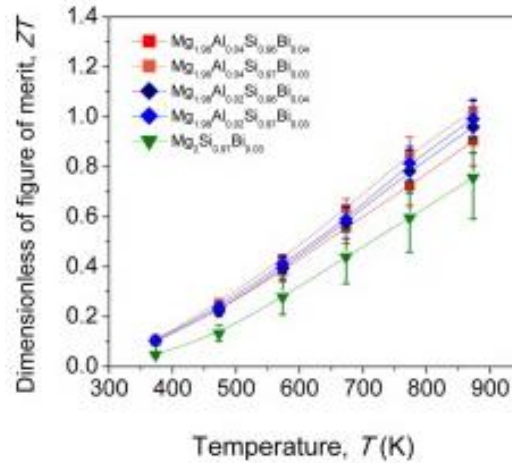
Figure 8: Temperature dependence of dimensionless figure of merit ZT for $Mg_{2-x}Al_xSi_{1-y}Bi_y$ (x = 0, 0.02, 0.04; y = 0.03, 0.04). Peak ZT is achieved at 1.02 at 873 K for $Mg_{1.96}Al_{0.04}Si_{0.97}Bi_{0.03}$. Reproduced from ref: [8]

Fedorov and co-workers [88] reported a ZT of 1.1 at 780 K for n-type $Mg_2Si_{0.4}Sn_{0.6}$ solid solutions. Zheng et al [80] fabricated Sb-doped $Mg_2Si_{0.4}Sn_{0.6}Sb_x$ solid solutions with combining mechanical alloying twice and SPS. They reported highest ZT of 1.40 of $Mg_2(Si_{0.4}Sn_{0.6})$ $Sb_{0.018}$ at 673 K. The significant enhance in the ZT is due to the decrease in lattice thermal conductivity by phonon scattering. Zhang and Zhao et al [89] doped $Mg_{2-x}La_x(Si, Sn)$ composites with La by in situ coating the Mg_2Si-rich bulk grain with Mg_2Sn-rich layer to increase the electrical conductivity and decrease the thermal conductivity. They achieved ZT ~0.82 at 810 K of $Mg_{2-x}La_xSi_{0.58}Sn_{0.42}$ composites with composition of x = 0.005. According to Zhang et al, further improvement of figure of merit can be done by optimising the compositional and microstructure of the composites in mid-temperature range. Yang et al [71] used SPS to synthesize the mixture of nanoscale and micro-size of 0.7 at% of Bi-doped Mg_2Si powders. According to Yang et al, the nanocomposite structure of Mg_2Si helps to reduce thermal conductivity and increase the Seebeck coefficient, though its nanograin hinders the electrical conduction. Overall TE performance is enhanced and a maximum ZT of 0.8 is achieved at 823 K. This result ~is 63% higher than Mg_2Si without nanocomposite structure.

2.2.1.2 SiGe-based TE materials

Since the last several decades, silicon germanium (SiGe) are considered as a significant thermoelectric material for elevated temperature applications. Hence, great attention has been paid in order to study the thermoelectric properties of this material. SiGe alloys possesses high mechanical strength, high melting point, low vapour pressure and good resistance to atmospheric oxidation [90]. Other advantages of SiGe alloys includes environmental friendly and low lattice thermal conductivity due to the addition of germanium in silicon matrix. The addition of Ge in Si will induce large differences in the mean free path between its electrons and phonons hence significantly reduce the thermal conductivity and increase the ZT. This material is currently the best thermoelectric material for power generation at high temperatures (~1173 K), therefore SiGe has been used in radioisotope thermoelectric generators (RTG) in space mission application and other elevated temperatures applications [9].
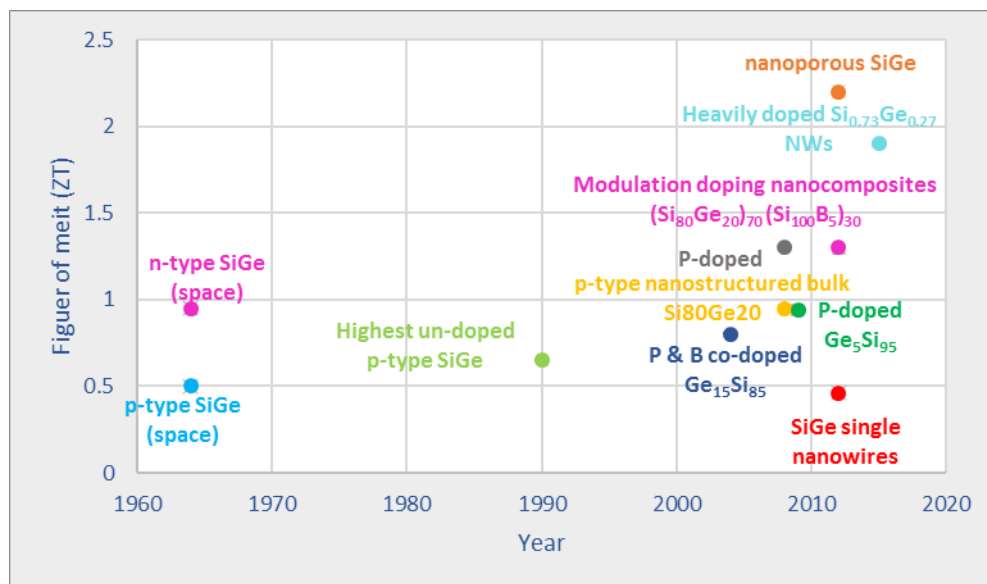
Figure 9: Overview of most promising of both p-type and n-type SiGe alloys from 1960 to 2015.

Since 1960s, several attempts have been done in order to increase the ZT in SiGe alloys, with peak ZT of n-type SiGe reaching 1 (~0.95) at 900-950°C. On the other hand, the maximum figure of merit of p-type SiGe remained pretty low [9]. Current space applications of p-type SiGe are reported to have a peak ZT of ~0.5 while the highest reported p-type SiGe achieved a peak ZT of ~0.65 [91]. Recently, significant enhancement of ZT in both p-type and n-type SiGe alloys have been achieved via nanostructuring approach by enhancing the phonons scattering at the grain boundaries to reduce the thermal conductivity [10, 91, 92]. Joshi et al [9] achieved ZT of 0.95 at 800-900°C in p-type nanostructured bulk $Si_{80}Ge_{20}$ doped with boron

powder, this achievement is around 50% enhancement compared to the previous highest record and ~90% enhancement compared to current used SiGe in radioisotope applications. According to Joshi et al, the significant enhancement of ZT is due to significant reduction of thermal conductivity due to the increased of phonon scattering from high density nanograin interfaces in the nanocomposite combined with the enhancement of power factor at elevated temperature.
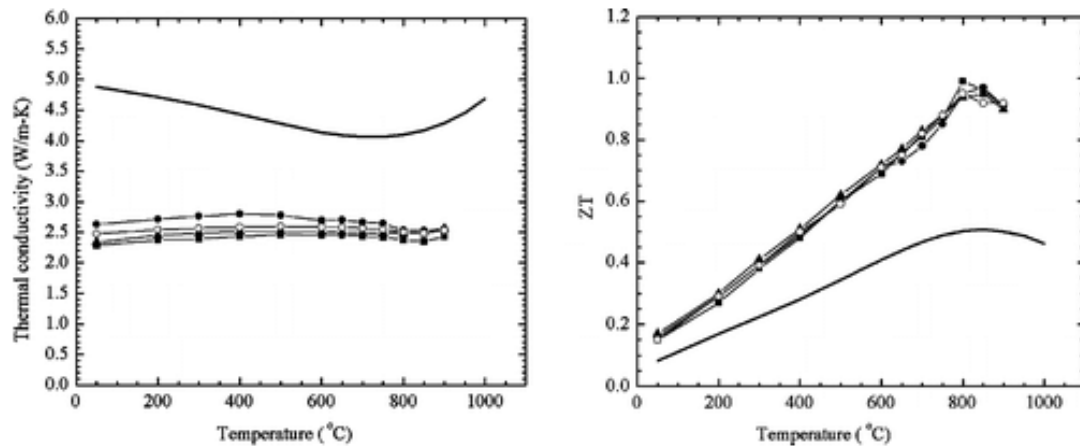
Figure 10: Dimensionless figure of merit (ZT)of 0.95 in p-type nanostructured bulk $Si_{80}Ge_{20}$ doped with boron powder, which is ~90% larger than currently used in space flight missions and 50% higher than the reported record I p-type SiGe alloys. The enhancement of the ZT is due to large decrease in the thermal conductivity due to increase of phonon scattering at grain boundaries as well as an increased in power factor at elevated temperature. Reproduced from ref: [9]

In the same period, Wang, Lee et al [10] added 2.0 mol % of phosphor into SiGe and synthesized with ball-milling and hot-pressing at 1000-1200°C. From the experiment, they reported a peak ZT of 1.3 at 900°C in n-type nanostructured $Si_{80}Ge_{20}P_2$, which is around 40% enhancement over the previous highest record of n-type SiGe (~0.93).
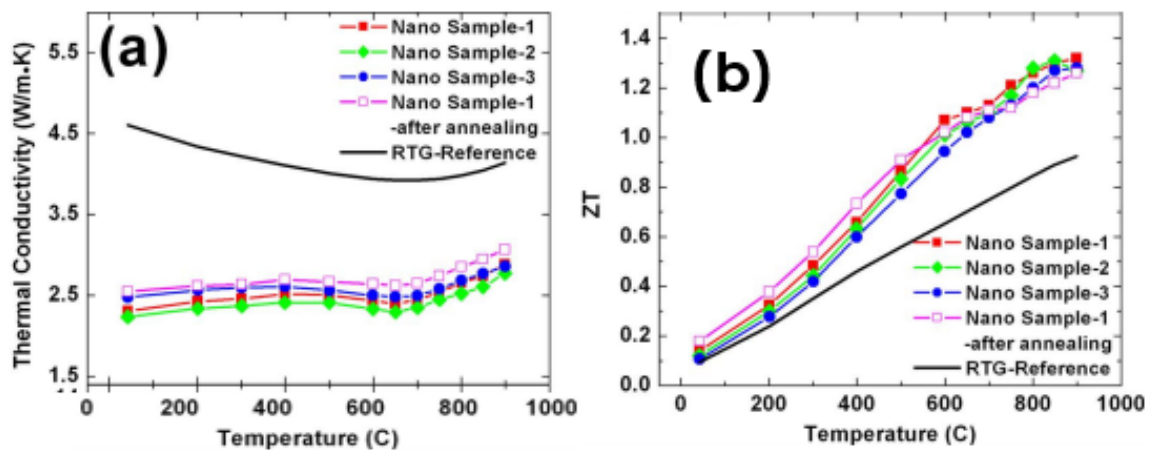
Figure 11: Temperature dependence of (a) the thermal conductivity, and (b) dimensionless ZT on both as-pressed nanostructured samples and RTG reference sample (solid line) after annealing at 1050ºC for 2 days in open air. Peak ZT of

In order to reduce the production costs and enhance the application properties, several attempts have been conducted to decrease the concentration of germanium due to the high cost and less abundance of germanium itself. Dismukes et al [93] used boron and phosphorus as dopants with 15% of Ge and 85% of Si. They calculated a maximum ZT of 0.8 for p-type $Ge_{15}Si_{85}$ alloy and ZT of 1 for n-type $Ge_{15}Si_{85}$ alloy at 1200 K. In 2009, Zhu et al [94] conducted an experiment by adding only 5 at % of Ge into Si matrix and doped with 2.5 at % of phosphorus by nanocomposite approach. They reported a ZT of ~0.94 at 900°C which is almost the same value as bulk SiGe achieved in RTG. According to Zhu et al, 5at % Ge is sufficient to reduce the thermal conductivity of n-type nano-Si by a factor of 2. The reduction in thermal conductivity is due to the enhancement of boundary phonon scattering. This achievement is quite significant considering only small amount of Ge is used hence reducing the total fabrication cost. However, if Ge is removed entirely, the maximum ZT of pristine nano-Si will reduce from 0.94 to 0.7 at 1000°C due to the trade-off between cost and thermoelectric performance of SiGe alloys [94, 95].

Another way to achieve high ZT in SiGe nanocomposites is through modulation doping approach. According to Yu and Chen et al [95], in the beginning, modulation doping was theoretically proposed and experimentally proved to enhance the power factor of nanocomposites $(Si_{80}Ge_{20})_{70}$ $(Si_{100}B_5)_{30}$ by mainly increasing the carrier mobility but not the ZT due to the increased in the thermal conductivity of the nanoparticles of pure silicon. In 2012, an alternative design of 3-D modulation doping is introduced by the same research group using $Si_{70}Ge_{30}$ alloy instead of pure Si as the nanoparticles and $Si_{95}Ge_5$ as the matrix to significantly increase the power factor while the thermal conductivity remained low, leading to peak ZT of ~1.3 at 900°C. The enhancement of power factor is due to the increased in electrical conductivity from the enhancement in carrier mobility and the lattice thermal conductivity remained low is due to the low thermal conductivity of the $Si_{70}Ge_{30}$ nanoparticles. Yu et al [95] also commented that the modulation-doping approach can be further enhanced by using a thin spacer layer to reduce the diffusion hence improving the measured performance.

Besides experimental approach, theoretical investigations on SiGe TE properties have been conducted by several research groups. In 2012, Lee et al [96] computed the TE properties of nanoporous SiGe and predicted ZT of 2.2 at 800 K and ZT of ~0.46 at the 450 K from single SiGe nanowires. This is achieved by simultaneously measuring the electrical, thermal

conductivity and the thermopower. According to Lee et al, the improvement in ZT is due to the significant decrease in the thermal conductivity to as low as ~1.2 W/m K at 450 K. Three years after that, Yi and Yu [97] proposed an improved models for predicting the thermoelectric properties of heavily doped SiGe NWs at wide range of temperature based on the Boltzmann transport equation with relaxation time approximation. The study of the SiGe NWs by Yi and Yu resulted in good agreement with the experimental data of both bulks and NWs of SiGe alloys. The maximum calculated results suggested a ZT of 1.9, 1.5, 1.2 and 0.8 is achieved at 800 K, 600 K, 450 K and 300 K respectively for optimum ionized impurity concentrations of $Si_{0.73}Ge_{0.27}$ NWs with 10 nm in diameter. These results summarized the possible direction of nanostructured SiGe-based thermoelectric materials to be used in future applications.

2.2.1.3 High manganese-based TE materials

Higher manganese silicide (HMS) is considered as a promising thermoelectric material due to its two naturally abundant elements in the Earth's crust, non-toxic and possess high Seebeck coefficient, low resistivity and high oxidation resistance at high temperature [98-100]. HMS belong to a family of Nowotny chimney ladder (NCL) phases with general structure of Mn_nSi_{2n-m} and is structurally related to $TiSi_2$ and $RuGa_2$ [11]. HMS are the only known compounds with the amounts of Si exceeding the Mn (63-53 at% of Si) [101]. Up to date, higher manganese silicide is represented by at least five phases: Mn_4Si_7, $Mn_{11}Si_{19}$, $Mn_{15}Si_{26}$, $Mn_{26}Si_{45}$, $Mn_{26}Si_{45}$ and $Mn_{27}Si_{47}$. These phases have similar properties and have tetragonal crystal structure with long C-axis as the Nowothy chimney ladder phases with energy gap of 0.4-0.7 eV [100].
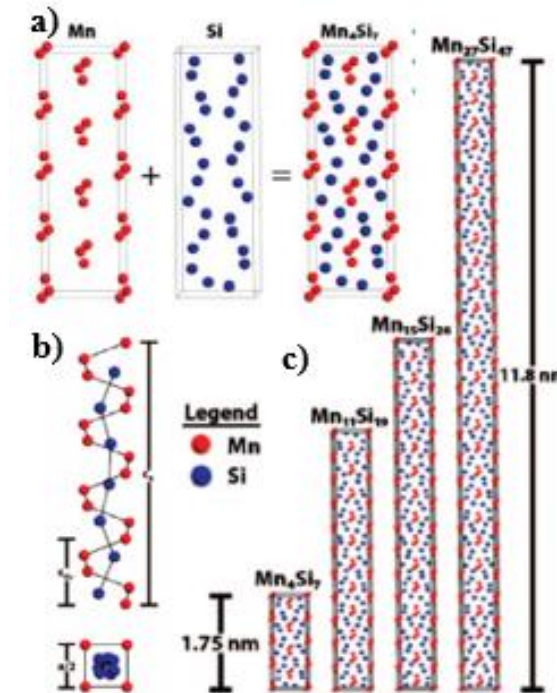
Figure 12: Crystal structures of Nowotny chimney ladder (NCL) phases of HMS and their comparison with TiSi2. (a) General NCL structure formed by the combination of one sub-lattice of transition metal atoms with the sub-lattice of main group atoms; (b) NCL structures of MnSi2-x with Si sub-lattice forming the ladder and Mn sub-lattice as the chimney; (c) Effects of the periodicity of sub-lattice on unit cell size for the four phases of HMS have completely characterized crystallographically with atomic positions. Reproduced from Ref. [11].

Due to the complex structure of HMS, the thermal conductivity of higher manganese silicides exhibits low and constant values between 2 and 4 W/m K from 300 K – 1000 K. Combination of low thermal conductivity and high power factor leading the ZT of ~0.4 at 800 K for un-doped HMS [101]. In 2014, Girard et al [102] reported un-doped single crystal of HMS by synthesizing high-purity MnSi-free single crystal of HMS by SPS and chemical vapour transport and achieved improvement in ZT of 0.52 ± 0.08 at 750 K. This achievement is due to the higher hole mobility owing to the high purity of HMS single crystal. Itoh and Yamada [103] synthesized Mn and Si by mechanical alloying, ball-milling and pulse discharge sintering under different conditions (at 200rpm for 36ks and 400 rpm for 36 ks). They reported mechanically alloyed $MnSi_{1.73}$ achieved max ZT of 0.47 at 873 K. Apart from single crystal HMS, several experiments on polycrystalline HMS have been attempted to achieve an improvement in the thermoelectric properties. An and Choi et al [100] synthesized polycrystalline HMS by SPS at 1123 K and achieved max ZT of 0.41. The high achievement in the figure of merit is attributed to the low thermal conductivity of polycrystalline HMS.

Various experiments and research have been conducted to improve the thermoelectric performances of HMS compounds such as doping with Al [104, 105], Ge [12], and etc. In 2011, Luo et al [105] reported a maximum ZT of 0.65 at 850 K (~40% higher than the un-doped sample) by doping HMS with Al. According to Luo et al, the addition of Al in HMS increases the carrier concentration and number of defects thereby increasing the electrical conductivity and lower the total thermal conductivity leading to an improvement in the ZT value. Ikuto et al [104] agreed with the reported results by Luo et al [105]. According to Ikuto, the doping of HMS with Al can improve the thermoelectric properties of bulk HMS by increasing the electrical conductivity from the increase in carrier density. They also added that Al doping will lower the thermal conductivity of the compounds.

In 2005, Aoyama et al [106] observed the effect of Ge doping on the morphology of MnSi in higher manganese silicides single crystal. They found that by addition of Ge into HMS single crystal, the volume concentration of MnSi shows initial increase and then decrease which is correlated to the change of TE properties. In 2009, Zhou et al [12] doped polycrystalline HMS with Ge by induction melting and hot-pressing and achieved maximum ZT of 0.6 at 833 K. According to them, the addition of 0.8% of Ge into HMS increases the electrical conductivity due to the enhancement of phonon scattering from the defects The dimensionless figure of merit of this optimized HMS polycrystalline has shown a 30% improvement compared to pure HMS compounds.
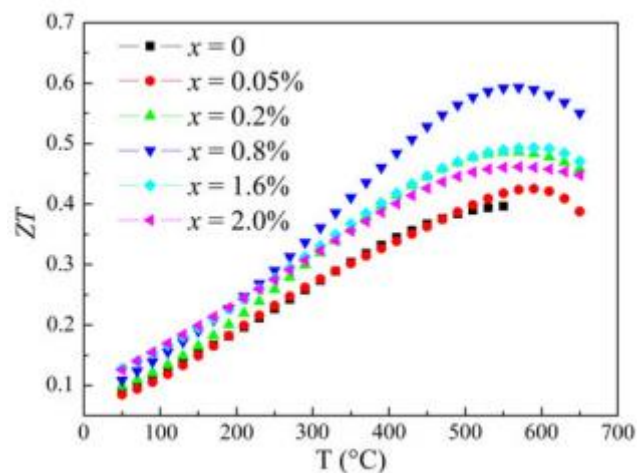
Figure 13: Temperature dependence of dimensionless figure of merit ZT of Mn(Si$_{1-x}$Ge$_x$)$_{1.733}$. Peak ZT of 0.6 is obtained at 833 K when x=0.8% due to an increased in the power factor and electrical conductivity from phonon scattering. This shown an improvement of >30% compared to pure HMS. Reproduced from ref: [12]

27

Apart from Al and Ge dopants, Ru is also used as dopants to HMS to tune the thermoelectric properties. Koyama et al [107] doped polycrystalline HMS with Ru to form $Ru_{1-x}Mn_xSi_{1.7}$. From the experiment, they reported maximum ZT of 0.76 at 880K by substituting Ru with Mn to form the $Ru_{1-x}Mn_xSi_{1.7}$ compounds. This is due to the significant increase in the power factor when the Mn content is kept at high amount (x > 0.75).

Norouzzudah et al [108] attempted to reduce lattice thermal conductivity of HMS by nanostructuring. They predicted the influence of grain size on the TE properties of HMS. According to them, ZT will be enhanced as long as the reduction in thermal conductivity due to the phonons scattering exceeded the reduction in the power factor due to enhancement of charge carrier scattering.

Although much research has been made in the study of HMS, for the thermoelectric applications, the ZT value (which is < 1) needs to be improved such as by tunning the carrier concentrations by doping, designing new preparation and synthesis methods, and optimizing synthesis conditions to reduce the unwanted side products that contaminates the compounds.

2.2.1.4 FeSi$_2$-based TE materials

Iron silicide is considered to have great potential as thermoelectric conversion devices for mid temperature range (230 – 630°C) without any driving mechanism [109]. Among several phases of iron silicide, semiconducting β- FeSi$_2$ has been widely known and well received as TE material for power generators, thermal sensor and optoelectronic applications since 1964 [110]. Semiconductor iron disillicide (β- FeSi$_2$) is one of the potential thermoelectric materials for high temperature range application due to it high resistance to oxidation, thermally stable, abundance as raw material and also its non-toxic properties [110, 111]. Other than that, it is also considered as one of the cheapest thermoelectric material [13]. However, compared to other non-environmental friendly materials such as Bi_2Te_3, PbTe and $CoSb_3$, the thermoelectric performance of β- FeSi$_2$ is not satisfying for practical applications [111]. To improve the thermoelectric performances of β- FeSi$_2$, various elements have been doped to iron disilicide during the experiment. In 1964, Ware and McNeill doped β- FeSi$_2$ with Co to obtained n-type β- FeSi$_2$. They found that the lattice thermal conductivity of the doped sample was decreasing with increasing of Co content. The reduction in the thermal conductivity was probably due to the point defect scattering. Similar test was performed by the same research group with Al as

dopants to form p-type β- $FeSi_2$. The results obtained were in good agreement as the n-type with the decreased of lattice thermal conductivity in the iron disilicide. However, due to the low solubility and high oxidation of aluminium, Al doping in semiconductor iron silicides is not widely used. Ur and Kim et al [109] conducted an experiment in 2002 by doping β- $FeSi_2$ with cobalt through mechanical alloying process and vacuum hot pressing. According to Ur et al, mechanical alloying materials will have a finer grain size hence may reduce the lattice thermal conductivity and improving the thermoelectric efficiency. From the results, both mechanical properties and thermoelectric properties (Seebeck coefficient and power factor) of n-type $Fe_{0.98}Co_{0.02}Si_2$ are significantly enhanced due to the β phase transformation and sintering effect during isothermal annealing.

In 1999, Watanabe and Hasaka [112] doped β- $FeSi_2$ (doping with 1 at % of either Mn or Co) into silver nitrate solution and sintered at 1373 K for 18 ks in vacuum. They examined the thermoelectric performance of the samples and reported that the power factor of β- $FeSi_2$-1 at% Co containing 3 at% of Ag was 6 times larger than the β- $FeSi_2$-1 at% Co at 573 K due to significant reduction of the electrical resistivity. Six years after that, Morimura et al [113] co-doped β-$FeSi_2$ with Ag and Co by induction melting and hot-pressing in vacuum. Their experimental results were in good agreement with Watanabe and Hasaka results. Morimura et al reported significant increase in the power factor due to the decrease in electrical resistivity by Ag addition. In 2003, Kim et al [114] reported that the ZT value of β- $FeSi_2$ prepared by powder metallurgy technique has improved from 0.19×10^{-4} K^{-1} (binary β- $FeSi_2$) to 1.3×10^{-4} K^{-1} by co-doping with Cr, Co and Ge. They reported max ZT of 1.3×10^{-4} K^{-1} in $Fe_{0.95}Co_{0.05}Si_{1.958}Ge_{0.042}$ at 845 K by decreasing the lattice thermal conductivity by addition of Ge and increasing the electrical conductivity by addition of all the dopants.

Although current highest achievement of iron disilicide has only maximum efficiency of ZT = 0.4 for n-type β-$FeSi_2$ and ZT=0.25 for p-type β-$FeSi_2$ [115, 116], it is still recognized as an important thermoelectric material due to the highly natural abundance of Fe and Si and also its environmental friendly material.

2.2.1.5 CrSi$_2$-based TE materials

Chromium disilicide ($CrSi_2$) is a hexagonal p-type silicides semiconductor with narrow band gap of $0.29 - 0.35$ eV [75, 117]. One specific features of chromium disilicide is its hole mobility

is 100 larger than its electron mobility. Due to the highly abundance of its constituent elements, good mechanical properties, non-toxicity, good oxidation resistance in air, thermal stability at high temperature and light weight, $CrSi_2$ is considered as a potential thermoelectric material for high temperature range application for waste heat recovery system [118, 119]. Although $CrSi_2$ exhibits good electrical conductivity ($\sigma = 10^5$ S m^{-1}) and thermopower (S = 100μVK^{-1} at 300 K), its large thermal conductivity (k = 10 Wm^{-1}K^{-1}) significantly lowers the figure of merit of $CrSi_2$. Maximum ZT of 0.2 - 0.25 at 600°C is achieved in un-doped $CrSi_2$ [119, 120]. Figure 14 shows the thermoelectric properties of un-doped $CrSi_2$. Several research has shown that the thermoelectric properties of thermoelectric materials can be enhanced significantly by doping. Fundamentally, doping increases the carrier concentration and decreases the lattice thermal conductivity of the material. As a result, the ZT value can be improved by proper control of doping. However, according to Fedorov [13], currently there are no papers available on the systematic study of the thermoelectric properties of doped $CrSi_2$. Pandey and Singh [119] used density functional theory to show that the defect transition levels from dopants can control the thermoelectric properties of doped $CrSi_2$. According to them, addition of Al or Mn dopants in $CrSi_2$ will increase the thermopower by lowering the overall carrier concentration. They also reported that higher thermopower is obtained in n-type rather than the p-type doped $CrSi_2$.

Varying the stoichiometry and composition is one of the way to enhance the figure of merit of $CrSi_2$. In 2013, Perumal et al [121] attempted to find the optimum composition from $CrSi_{2-x}$ ingots (with 0< x < 0.1) at 300 to 800 K to improve the thermoelectric performance. They reported that the electrical resistivity and Seeback coefficient is significantly decreased when x > 0.04 (silicon deficiency) due to the formation of metallic secondary phase in $CrSi_2$ matrix phase, while the total thermal conductivity of $CrSi_{2-x}$ samples is minimum when the x = 0.04 and continue to decrease when Si deficiency is increased. As a result, peak ZT of 0.1 is observed at 650 K for $CrSi_{1.98}$. In the same period, the same research group attempted to co-substitute Mn and Al with polycrystalline $CrSi_2$ by substituting Mn at Cr site and Al at Si site at temperature range of 300 to 800 K by arc melting (in Ar atmosphere) and hot-pressing [122]. From the results, they found that the lattice parameters are increasing with Mn and Al contents. The presence of Al atoms in Si site decreases the electrical resistivity of $Cr_{1-x}Mn_xSi_{2-x}Al_x$ solid solution due to the increase in hole carrier density. The Seebeck coefficient also decreases with increasing of Al concentration due to the decrease of hole mobility, while with Mn dopant, the Seebeck coefficient remained the same. Co-substitution of Mn and Al have also significantly decreases the total thermal conductivity of $Cr_{1-x}Mn_xSi_{2-x}Al_x$ solid solution hence the figure of

merit is enhanced to ZT = 0.13 for x = 0.1. This value has increased >40% compared to pure un-doped $CrSi_2$ (ZT ~0.09).
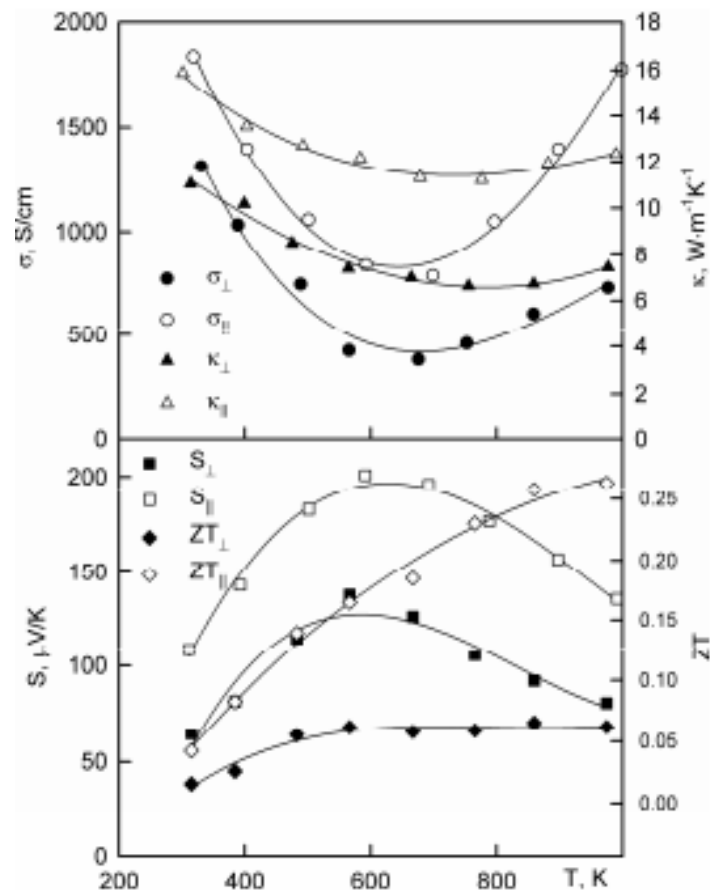
Figure 14: Thermoelectric properties of un-doped $CrSi_2$. Reproduced from Ref. [13]

According to Perumal et al [118], there are several approaches to process $CrSi_2$: (i) formation of precipitates/lamellar patterns via solid state phase transformation at very high driving force, (ii) rapid solidification by melt-spinning, (iii) solution-synthesis routes for nanocomposites and nanocrystallized bulk materials, (iv) mechanical alloying (MA) via high energy ball-milling followed by hot pressing or SPS. However, the high melting point of CrSi2 (> 1490°C) makes the melt-spinning, solid state phase transformation and tailoring nanostructure of $CrSi_2$ not possible. Hence, only mechanical alloying approach with ball-milling or SPS are the most appropriate way to process $CrSi_2$. Kajikawa et al [123] combined SPS and hot pressing approach to process $CrSi_2$ at 1573 K. They observed non-dimensional ZT of 0.45 and 0.59 at 900 K for SPS and SPS + hot pressing approach of $CrSi_2$ thermoelectric materials due to the reduction of hole concentration and phonon scattering by SPS processing. Dasgupta and Umarji [124] synthesized $CrSi_2$ via mechanical alloying at high speed to minimised the impurity contamination from iron that will cause the decrease in ZT value. They reported peak ZT of

0.2 at 600 K by increasing the milling speed to 500 rpm. This obtained value has shown an increase of ZT compared to the arc melting method.

Other approaches such as single crystal $CrSi_2$ nanowires were still on investigation for their effects on the enhancement of ZT on future thermoelectric applications [125, 126].

2.2.1.6 Ru_2Si_3--based TE materials

Semiconductor ruthenium silicide (Ru_2Si_3) that can be grown in epitaxial direction on silicon, has received attention from researcher in the prospects of high temperature space power applications in thermoelectric materials [127]. Ruthenium silicide is similar to iron disilicide with phase transition at 967^oC [128]. In low temperature range, ruthenium silicide is in alpha phase (α- Ru_2Si_3) with orthorhombic structure while in high temperature range, ruthenium silicide has beta phase (β- Ru_2Si_3) with tetragonal structure. Both of the alpha and beta phases are semiconductor materials [13]. Fedorov M. I [13] also added that crystal structure of Ru_2Si_3 is similar to high manganese silicide with plate-like precipitates. In terms of the directional axis, in the reference of β- Ru_2Si_3 by Poutcharovsky et al [129], the plate-like precipitates of Ru_2Si_3 were orthogonal to [010] axis while according to Souptel et al [130], the precipitates were orthogonal to either [100] or [001]. Figure 15 and 16 below shows the thermoelectric properties of crystal structure of Ru_2Si_3 with [010] direction measured by Simkin et al [14]. According to Simkin et al, p-type Ru_2Si_3 with [010] direction has superior thermoelectric properties which is consistent with its band structure models. N-type doped Ru_2Si_3 has higher Seebeck coefficients along the [001] orientation axis, while thermal conductivity is not strongly dependent on the sample orientation much.
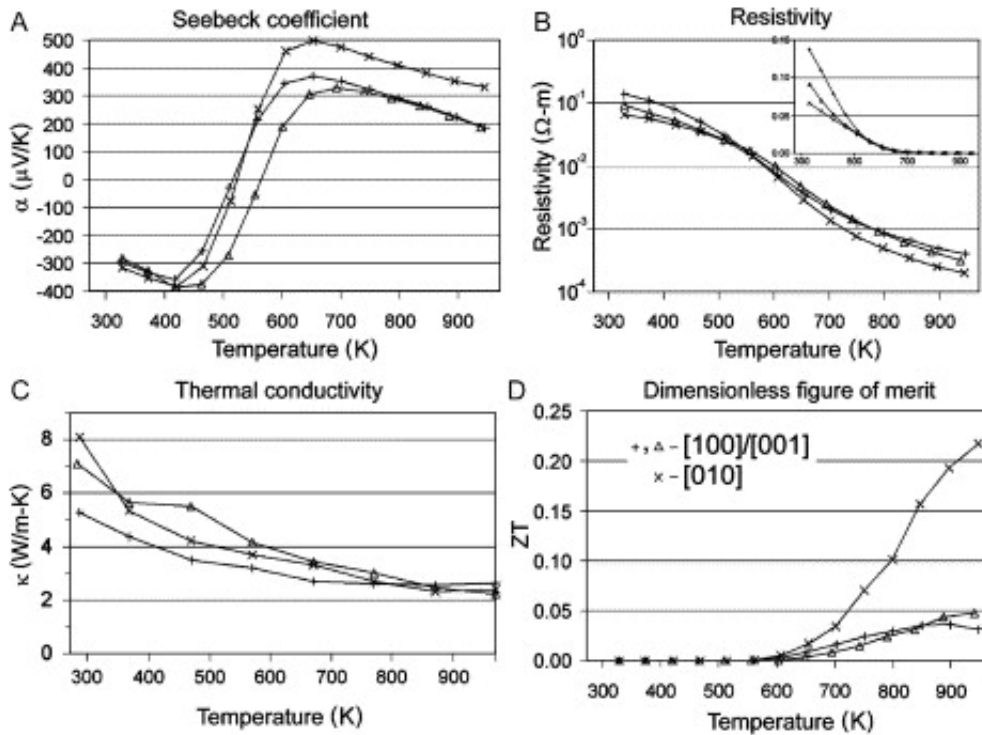
Figure 15: Measured TE properties of as grown crystalline of ruthenium silicide: a) Seebeck Coefficient; b) electrical resistivity; c) thermal conductivity; d) calculated dimensional figure of merit ZT. Reproduced from ref: [14]
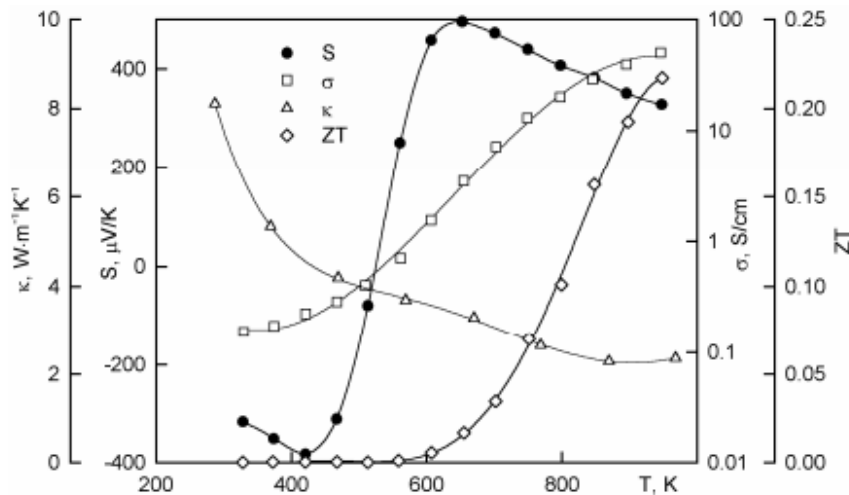
Figure 16: Thermoelectric properties of ruthenium silicide in [010] direction. Reproduced from ref: [13]

Thermoelectric ruthenium silicide has high thermal stability, high resistance to chemical exposure hence it is highly applicable to be used in elevated temperature space applications similar to SiGe. According to C.B Vining in his conference paper in 1992 [131], un-doped single crystal of ruthenium silicide was grown and analysed theoretically. Vining stated that the possibility of Ru_2Si_3 to achieve higher figure of merit compare current state-of-art SiGe.

Furthermore, Vining and Allevato [132] added that p-type Ru_2Si_3 has the potential for improvement in the figure of merit ZT of a factor of 3 and n-type Ru_2Si_3 may be 50% better than current SiGe standard. Despite that, current experimental efforts to achieve ZT> 1 have not yet successful due to the poor quality of the specimen used [127]. Therefore, in order to obtain higher values of figure of merits ZT, dopants must be identified and added for both p and n-type Ru_2Si_3.

In 2003, Ivanenko et al [15] doped single crystal Ru_2Si_3 with Mn by floating zone method and studied its behaviour theoretically and experimentally. According to Ivanenko et al, experimentally, the electrical resistivity of Mn-doped Ru_2Si_3 is much lower than the undoped single crystal. Other than that, doping with Mn has increase the carrier mobility by a factor of two compared to undoped pristine Ru_2Si_3. While in theoretical estimation, there are slight difference between the charge carrier mobility especially in the temperature range of 300 to 500 K. Figure 17 below shows the obtained results of effect of Mn doping on the thermoelectric properties of Ru_2Si_3.
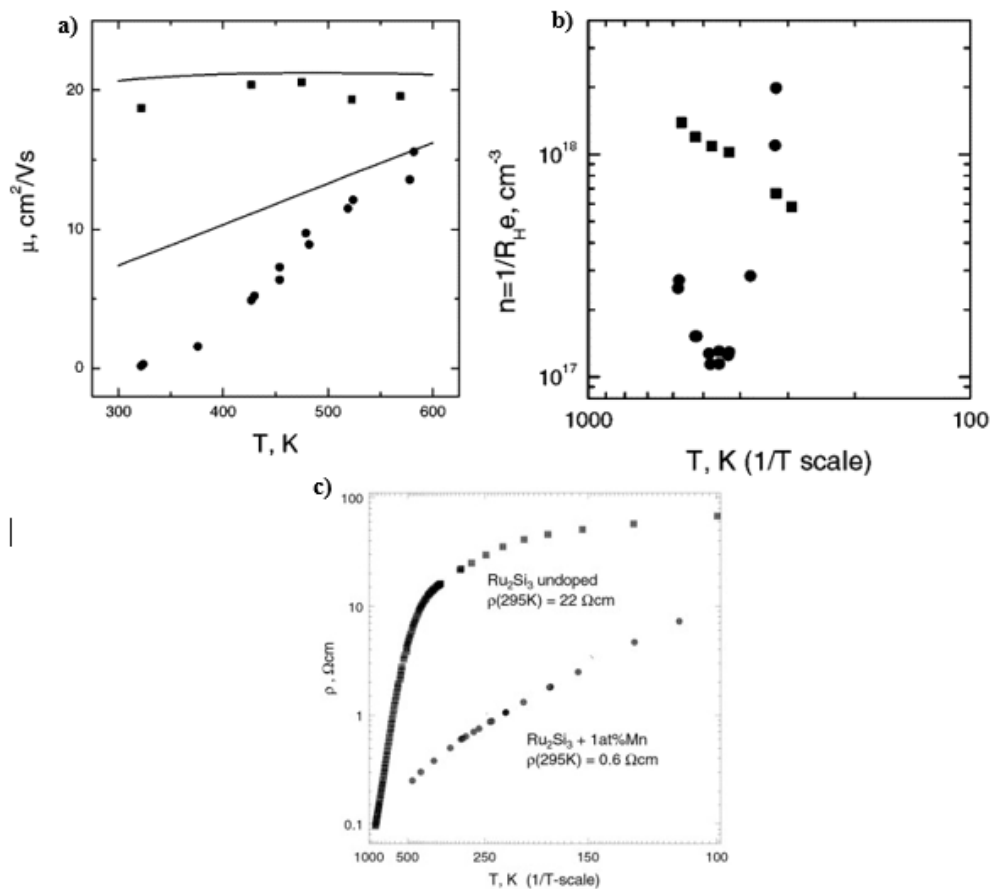
Figure 17: Temperature dependence of: a) carrier mobility; b) carrier concentration; c) electrical resistivity in un-doped (circles) and Mn-doped (squares) Ru₂Si₃ single crystal. Reproduced from ref:[15]

In another paper published by Ivanenko et al [133] in 2004, they found that pure Mn-doped of Ru$_2$Si$_3$ has achieved Seeback coefficient with twice larger values than corresponding un-doped Ru$_2$Si$_3$ in room temperature. The highest dimensionless figure of merit (ZT) obtained at 800 K is calculated to be 0.2 and 0.27 for un-doped and Mn-doped Ru$_2$Si$_3$. Krivosheev et al [127] did the similar experiment as Ivanenko by doping Ru$_2$Si$_3$ with manganese by zone arc melting combines with optical heating. Table 3 below shows the comparison of the thermoelectric properties obtained from their experiments.

TE properties	Un-doped	Mn-doped	Comments
Electrical resistivity	22 Ω	15 Ω	Increasing the carrier mobility
Seebeck coefficient	300 µV/K	400 µV/K	Negative Seebeck for un-doped sample and positive Seebeck for Mn-doped at 500 K.
Thermal conductivity	5 W/ K m	5 W/ K m	At room temperature, the thermal conductivity of un-doped and doped sample are similar. However, at temperature below 100 K, thermal conductivity of doped sample is much higher than un-doped one.
ZT	0.2	0.3	Mn-doped has higher ZT due to higher Seebeck coefficient.

Table 3: Comparison of thermoelectric properties of un-doped and Mn-doped single crystal of Ru$_2$Si$_3$.

Using the similar floating zone and arc melting methods, Arita et al [16] doped Ru$_2$Si$_3$ with ruthenium-rhodium-silicon (Ru$_{1.92}$Rh$_{0.08}$Si$_3$) and compared their thermoelectric properties with un-doped sample. According to them, floating zone sample has higher ZT due to its high improvement in the electrical conductivity especially in n-type Rh-doped Ru2Si$_3$. The comparison between figure of merit for n-type and p-type doped Ru$_2$Si$_3$ is shown in figure 18 below.
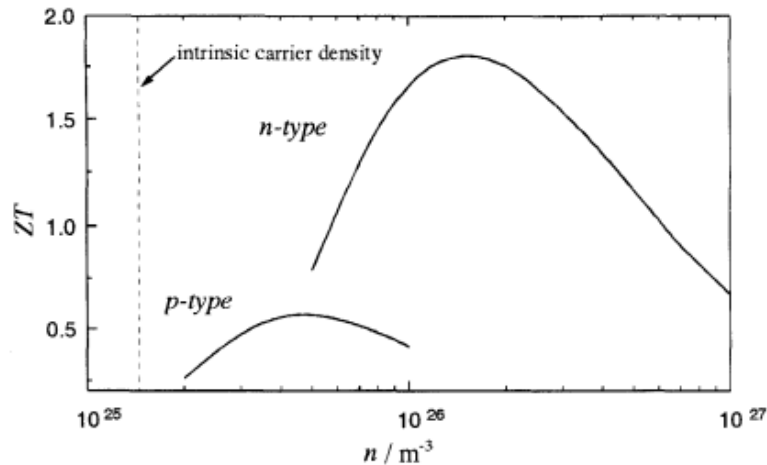
Figure 18: Calculated figure of merit ZT for Rh doped Ru₂Si₃ as a function of carrier density. Reproduced from ref:[16]

Apart from manganese and rhodium, titanium is also used as dopants to obtain higher thermoelectric properties. Vining and Allevato [132] doped Ru_2Si_3 with Ti by growing on the stoichiometric melts in boron nitride crucibles using Bridgeman-like methods for synthesis. Based on the results obtained, titanium doping has successfully decreased the electrical resistivity when T>500 K, this result is similar as what Mn dopants did as mentioned earlier. However, the obtained hall coefficient was unusual especially when the temperature is below 500 K. Due to that, carrier concentration calculated from hall coefficient has unusual values.

The effects of different dopants and synthesis methods were discussed in the paragraph earlier from a number of papers [13-16, 107, 127, 129, 132]. Due to several samples used, most of the results have extrapolation elements for the calculation of their dimensionless figure of merit. Nonetheless, a complete study for this type of silicide has not been accomplished yet.

2.2.1.7 Cobalt monosilicide-based TE materials

Cobalt monosilicide is an n-type semi metallic, abundant, low cost and environmental friendly thermoelectric material for mid-range temperature applications (200-700°C). It is regarded as potential thermoelectric materials due to its high electrical conductivity (1 m Ω cm) and decent Seebeck coefficient (~80 μ V/K at 300 K). The power factor of CoSi is relatively similar to those observed in the state-of-the-art TE materials such as bismuth tellurite [17, 18, 134]. Furthermore, the calculations of its band-structure shows narrow band gap indicating its potential as good thermoelectric materials [135]. However, the thermal conductivity of CoSi is too high to achieve optimum ZT to be used in commercial applications. In order to enhance the

thermoelectric performance and increase the overall ZT, several strategy can be optimized: increases the charge carriers by adding different dopants; enhancement of phonon scattering by promoting crystallographic disorder; and nanostructuring [17, 18, 134, 135].

Nanostucturing has been widely used to increase the TE performance by lowering the lattice thermal conductivity from reduction of lattice contribution [17]. According to Bux et al [70], nanostructuring has managed to reduce the lattice thermal conductivity of doped Si materials by 90%. Although nanostucturing has successfully enhanced ZT of some TE materials such as Mg_2Si, $CrSi_2$ and SiGe, the effect of nanostructuring on the thermoelectric performance of CoSi have yet been investigated much. A few widely used of nanostructuring techniques includes mechanical alloying, SPS or arc melting [17, 134]. He et al [136] synthesize CoSi by mechanical alloying and investigated on the CoSi properties and compositions. Longhin et al [17] commented that shorter milling time during the synthesis process will obtain less contaminations and smaller crystal of CoSi. Longhin and group has successfully proved the effectiveness of using MA technique by obtaining pure and homogenous powder from CoSi ingots. Furthermore, the thermal stability of nanostructured CoSi was achieved in the mid-range temperature applications.

Figure 19 below shows the obtained TEM images of mechanical milling of CoSi powders by Longhin et al. The analysis from TEM confirmed the nanostucturing of the CoSi grains with the dimension of the powder range from 6 nm to 6 micrometers. Particles with small grain size (nm) are usually consist of single-crystal while particles larger than 30nm usually are considered as poly-crystalline. The dark-field images on figure 12 (c) shows the identification of different types of crystalline in the clusters.
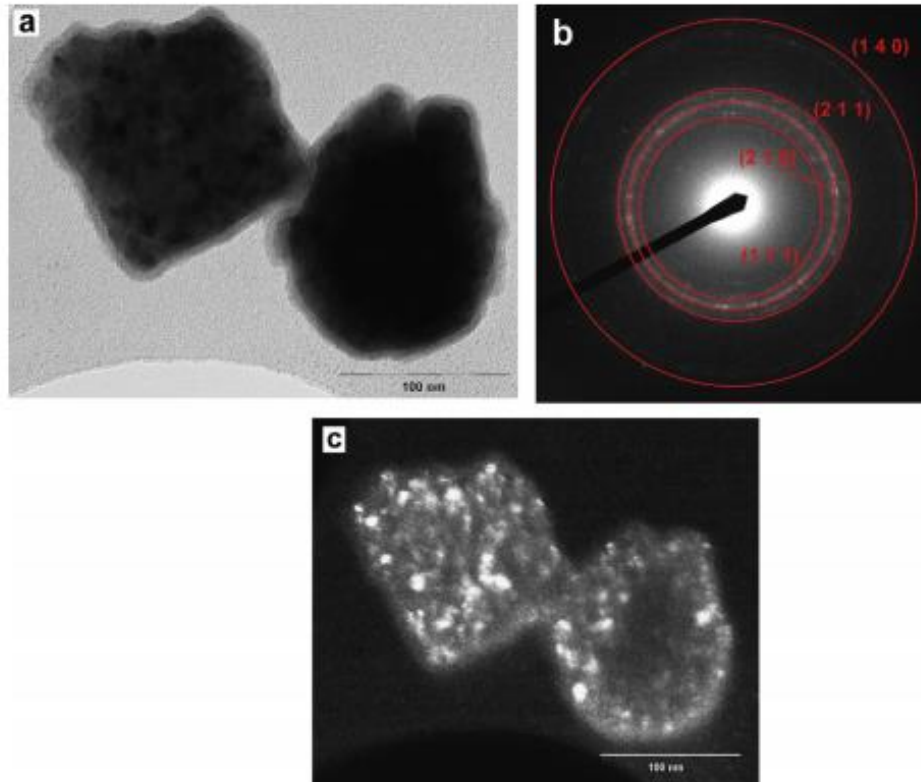
Figure 19: Images of nanometric arc-melted MM powders obtained from TEM: a) multi-crystal agglomerate, b) within the selected area of diffraction pattern, c) Dark-field image. Reproduced from ref: [17]

One year after, the same research group led by Longhin [134] performed nanostucturing of CoSi by spark plasma sintering (SPS). They managed to reduce the total thermal conductivity by 35% from SPS treatment. However, this led to an increase in the grain boundary density hence lowers the electrical conductivity of CoSi nanostructured material. From the results obtained, Longhin et al commented that the probability of increasing the electrical conductivity can be enhanced by adding small amounts of boron to segregate the grain boundaries hence increase the electrical conductivity and overall ZT values.

Other than nanostructuring, several attempts have been conducted to increase the thermoelectric performances of CoSi. In 2006, He et al [136] used hydrogen storage alloys of CoSi prepared by ball milling in aqueous KOH solution and examined the thermoelectric properties. Hsu et al [135] investigated the effects of partial substitution of germanium for Si on the binary compounds of CoSi. According to Hsu et al, doping of Ge in CoSi enhances the lattice phonon scattering by point defect scattering which led to an enhancement in the thermoelectric performances and ZT value by increasing the power factor and lowering the total thermal conductivity.

Similarly to what has been conducted by Hsu et al, Lue et al [18] partially substituted Al to CoSi binary compounds and analysed the changes in the thermoelectric properties. From the experiments, they found that the substitution of 15 % of Al in Si has significantly reduced the electrical resistivity (by 20 times) by increasing the hole carriers. Other than that, doping of Al in CoSi has changed the sign of the Seebeck coefficient from negative to positive. Furthermore, Al substitution introduced point defects scattering hence significantly lower the lattice thermal conductivity and improving the total dimensional figure of merits. Figure 20 below shows the obtained results of the thermoelectric properties of $CoSi_{1-x}Al_x$ when (x=0-0.015).
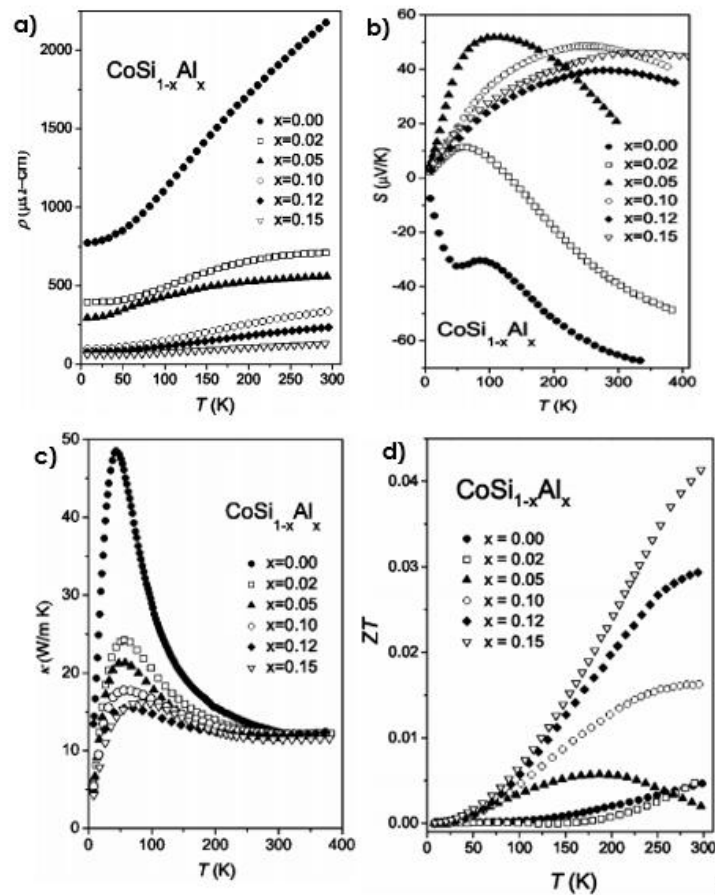
Figure 20: a) Electrical resistivity, b) Seebeck Coefficient, c) total thermal conductivity, d) Dimensionless figure of merit of $CoSi_{1-x}Al_x$ as a function of temperature. Reproduced from ref: [18]

In order to further enhance the thermoelectric properties of CoSi single crystal, co-doping approach was performed by several research groups. In 2006, Pan et al [137] co-doped CoSi single crystal with aluminium and phosphor and compared the TE properties with undoped sample. Based on the theoretical calculations of the electronic structure, they found that by increasing the Al and P concentration on CoSi sample, there are significant increase in the density of hole carriers hence decreasing the electrical resistivity. From this, Pan et al

commented on the high possibility of increasing the overall dimensionless figure of merit bu this co-doping. However, due to limited data obtained, the exact ZT enhancement have yet to be obtained.

Due to limited research papers published on this type of thermoelectric material and less popularity compared to Mg_2Si, HMS or SiGe, the overall summaries of cobalt monosilicide are only limited to several research groups and mostly conducted from complex theoretical calculations.

2.2.1.8 Rhenium silicide -based TE materials

Similar to other types of silicide materials, rhenium silicide ($ReSi_{1.75}$) is considered as potential thermoelectric materials for microelectronic applications [20]. Rhenium silicide has small band-gap varying from 0.11-0.36 eV [115, 138]. The thermoelectric properties of rhenium silicide are highly anisotropic with p-type behaviour measured along [100] and n-type behaviour measured along [001] for single crystals [19]. The Seebeck coefficient of $ReSi_{1.75}$ along the [100] is moderate (150-200 μ V/K), but when it is along [001] direction, the Seebeck increase to ~250-300 μ V/K. Due to that, high ZT value of 0.7 (n-type) are achieved at 800°C when it is measured along [001] direction while ZT of 0.2 are achieved at [100] direction (p-type). [19].

Rhenium silicide ($ReSi_{1.75}$) has monoclinic crystal structure with organized arrangement of the Si vacancies in the underlying $C11_b$ structure (with lattice parameters of a= 0.3139 nm, b=0.3121 nm, c= 0.7670 nm and β=89.97°). Figure 21 shows the $C11_b$ structure of $ReSi_{1.75}$.
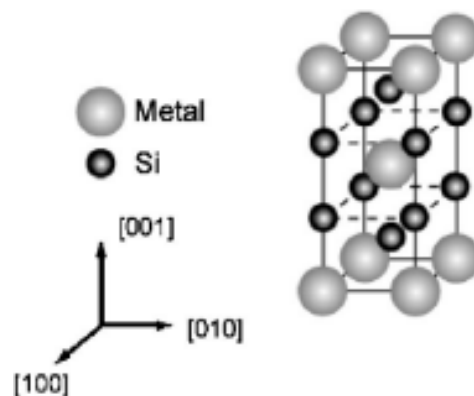
Figure 21: Unit cell of $C11_b$ structure. For rhenium silicide, some of the Si atoms are absent from their original positions. The Si vacancies are organized in order in the unedrlying $C11_b$ structure. Reproduced from ref: [19]

In 2003, Harada et al [139] investigated the effects of Mo doping on crystal structure and TE performances of $ReSi_{1.75}$. Based on the results obtained, they found that the concentration of silicon vacancies was significantly decreased by increasing of Mo contents. Additional of 2% Mo has managed to obtain ZT of 0.8 at 1073 K. Three years after, Haruyuki [140] investigated the TE properties of binary and ternary of $ReSi_{1.75}$ with Mo as dopant as well. The result obtained was in agreement with Harada et al, for binary case, ZT of 0.8 is achieved for n-type $ReSi_{1.75}$ due to extensive shear operation on its nano-scale.

Qiu et al [20] carried out theoretical studies and calculations on Al and Mo doped $ReSi_{1.75}$. The results obtained were similar with Harada et al and Haruyuki, they found that the power factor along [100] direction for p-type doped $ReSi_{1.75}$ and [001] direction for n-type doped $ReSi_{1.75}$ are significantly larger compared with un-doped $ReSi_{1.75}$ compounds. Although the lattice thermal conductivity was found to be independent of doping, large decrease in the power factor has significantly enhanced the figure of merit of $ReSi_{1.75}$ compound.

Other than doping, synthesis techniques were used to improve the thermoelectric performances of $ReSi_{1.75}$. Filonov et al [141] used floating-zone melting method to grow un-doped and Al-doped single crystal of $ReSi_{1.75}$ to study the thermoelectric properties theoretically and experimentally. Although the highest Seebeck coefficient for undoped and Al-doped sample are 130 μ V/K and 100 μ V/K at 800 K which contributed to low ZT value, Al-doped $ReSi_{1.75}$ sample has successfully decrease the electrical resistivity by 3 fold compared to undoped sample. The precise data of figure of merit was not included in the paper, however, due to low electrical resistivity, the possibility of enhancing the figure of merit is high.
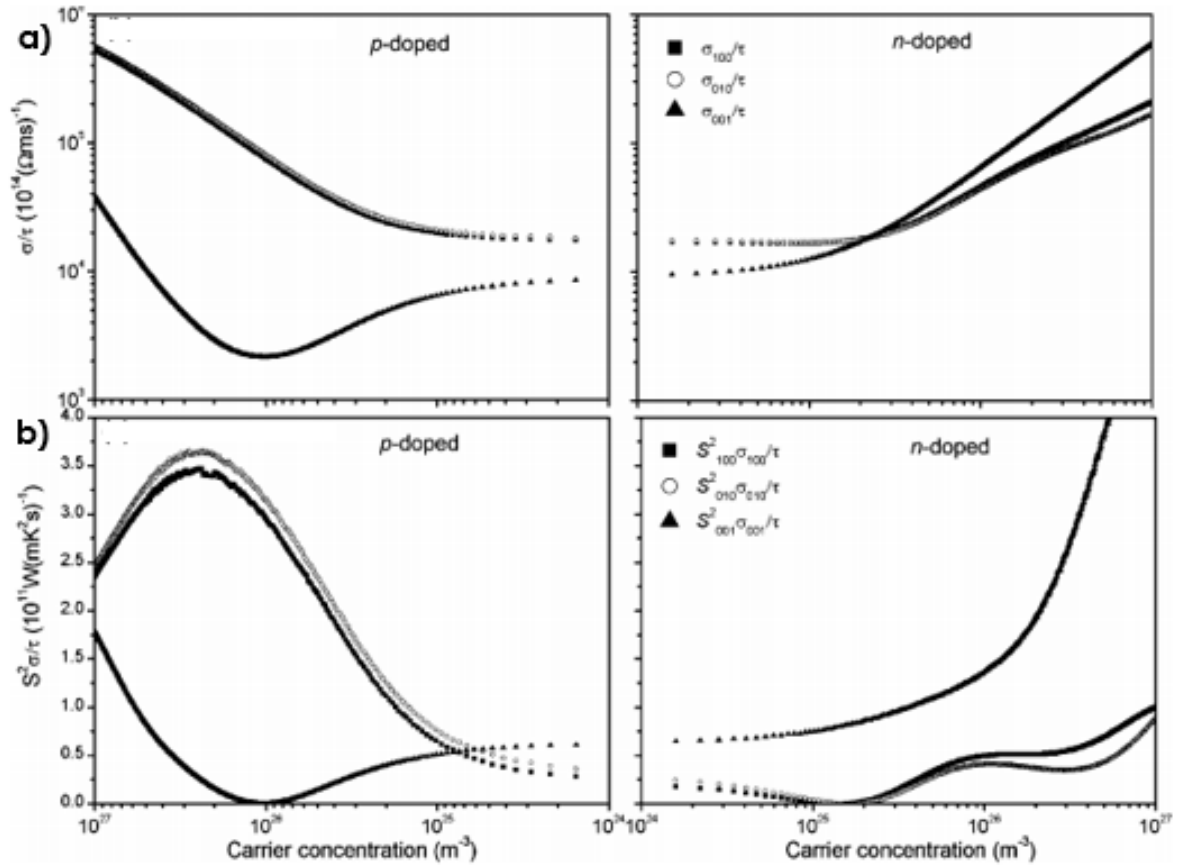
Figure 22: Thermoelectric properties at different axis directions calculated from the band structure of ReSi$_{1.75}$ at 600 K as a function of carrier concentration; a) electrical conductivities relatives to relaxation time, b) power factor relative to relaxation time as a function of doping. Reproduced from ref: [20]

Chapter 3: Conclusion

Silicides are one of the most promising thermoelectric materials in current industry due to their low cost, environmental friendly, highly abundance and the ability to achieve high thermoelectric figure of merit. High ZT that was achieved by those state-of-art thermoelectric materials such as Bi$_2$Te$_3$ and PbTe can be achieved in Mg$_2$Si, SiGe and HMS silicide materials. The probability of achieving higher ZT in silicide based materials can be enhanced by optimum alloying and doping in single or polycrystalline material. Lower band gap silicide such as CrSi$_2$ and ReSi$_2$ are receiving slightly less attention, however current research has increased the possibility of turning those material into advantageous thermoelectric materials for commercial applications.

Ru$_2$Si$_3$ are important semiconductor material due to its ability to be used in high temperature applications such as in space power application. However, currently too little information that are available regarding their thermoelectric performance in order to estimate the ZT values.

Other silicide such as germanides (SiGe) are expected to achieve higher figure of merit. Although germanides tend to have small band gaps that restrict their usage in some applications, they possess low thermal conductivity, high mechanical strength and high melting point which enabled their application in elevated temperature such as radioisotope TE generators in space application.

Based on the summary above, the study for silicides thermoelectric material still require a lot of improvement in order to achieve satisfying ZT values. Some of the silicide has achieved high figure of merit while others possess high anisotropic properties that are significant in anisotropic applications. Hence, fully understanding on the behaviour of these aspects can lead to further improvement on its thermoelectric performances.

Chapter 4: Outlook and Future Challenge

Environmental friendly thermoelectric materials provide solution for current energy crisis and environmental pollution. However, the conversion of thermoelectric efficiency is still low and only limited to the laboratory experiment instead of commercial applications. In order to be commercialised, the efficiency must be > 40% or ZT must be > 3. To reach ZT of greater than 3, it would be difficult and complicated as it will need impressive increase in the power factor by enhancing the electrical conductivity and lowering the total thermal conductivity.

Although new technique and technology were implemented to enhance the dimensionless figure of merit and thermoelectric efficiency, other issues and difficulties regarding the new innovation will need to be overcome. For example, by promoting distortion on the density of states and band convergence can increase the carrier effective m* and Seebeck coefficient as well, however this will result in large decrease in the carrier mobility. As mentioned in chapter 2, one way to increase the thermoelectric performances is through nanostructuring approach. Using nanostructuring, total thermal conductivity can be decreased, however decreasing the thermal conductivity will enhance the carrier scattering.

Other challenge is to implement the thermoelectric waste heat recovery technology into industrial applications. In order to fulfil this, continuous effort in the research for more efficient

and inexpensive thermoelectric materials must be conducted. Furthermore, it must be non-toxic and sustainable. Silicides based thermoelectric materials have been acknowledged as one of the most promising materials for this applications. Furthermore, some silicides such as SiGe has pinpointed itself as thermoelectric material with reasonable ZT to be used in space RTG applications. Magnesium silicide based are believed to be a promising material for the next generation of TE materials for waste-to-heat recovery systems especially in automotive industry. It is highly abundant, light weight non-toxic material which is significant for the application in transportation field. One drawback of this material is the limitation to be used at high temperature applications.

Other materials apart from silicide such as oxide and organic thermoelectric materials have gain large interest as a potential candidate for future thermoelectric application. With the growing in technologies, new and better techniques in the nanostructuring might be able to develop higher thermoelectric efficiency in the future.

Chapter 5: Reference

1. Wikipedia, *Heavy metal (chemical element)*.

2. He, J., Y. Liu, and R. Funahashi, *Oxide thermoelectrics: The challenges, progress, and outlook.* Journal of Materials Research, 2011. **26**(15): p. 1762-1772 %R doi:10.1557/jmr.2011.108.

3. Snyder, G.J. and E.S. Toberer, *Complex thermoelectric materials.* Nat Mater, 2008. **7**(2): p. 105-114.

4. Vaqueiro, P. and A.V. Powell, *Recent developments in nanostructured materials for high-performance thermoelectrics.* Journal of Materials Chemistry, 2010. **20**(43): p. 9577-9584.

5. Ratai, E., M.P. Augustine, and S.M. Kauzlarich, *Synthesis and Characterization of the Mg2SixGe1-x Solid Solution.* The Journal of Physical Chemistry B, 2003. **107**(46): p. 12573-12577.

6. U S Geological Survey. *Rare Earth Elements—Critical Resources for High Technology*. 2005; Available from: http://pubs.usgs.gov/fs/2002/fs087-02/.

7. Hu, X., D. Mayson, and M.R. Barnett, *Synthesis of Mg2Si for thermoelectric applications using magnesium alloy and spark plasma sintering.* Journal of Alloys and Compounds, 2014. **589**: p. 485-490.

8. Kim, G., et al., *Co-doping of Al and Bi to control the transport properties for improving thermoelectric performance of Mg2Si.* Scripta Materialia, 2016. **116**: p. 11-15.

9. Joshi, G., et al., *Enhanced thermoelectric figure-of-merit in nanostructured p-type silicon germanium bulk alloys.* Nano Letters, 2008. **8**(12): p. 4670-4674.

10. Wang, X.W., et al., *Enhanced thermoelectric figure of merit in nanostructured n-type silicon germanium bulk alloy.* Applied Physics Letters, 2008. **93**(19): p. 193121.

11. Higgins, J.M., et al., *Higher Manganese Silicide Nanowires of Nowotny Chimney Ladder Phase.* Journal of the American Chemical Society, 2008. **130**(47): p. 16086-16094.

12. Zhou, A.J., et al., *Improved Thermoelectric Performance of Higher Manganese Silicides with Ge Additions.* Journal of Electronic Materials, 2009. **39**(9): p. 2002-2007.

13. M.I., F., *Thermoelectric silicides: past, present and future* Journal of Thermoelectricity, 2009. **2**.

14. Simkin, B.A., Y. Hayashi, and H. Inui, *Directional thermoelectric properties of Ru2Si3.* Intermetallics, 2005. **13**(11): p. 1225-1232.

15. Ivanenko, L., et al., *Transport properties of Mn-doped Ru2Si3.* Microelectronic Engineering, 2003. **70**(2–4): p. 209-214.

16. Arita, Y., T. Miyagawa, and T. Matsui. *Thermoelectric properties of Ru$_2$Si$_3$ prepared by FZ and arc melting methods*. in *Thermoelectrics, 1998. Proceedings ICT 98. XVII International Conference on*. 1998.

17. M, L., et al., *Nanostructuration of CoSi by mechanical milling and mechanical alloying.* Solid State Sciences, 2014. **38**: p. 129-137.

18. C. S. Lue, Y.-K.K., C. L. Huang, and W. J. Lai, *Hole-doping effect on the thermoelectric properties and electronic structure of CoSi.* PHYSICAL REVIEW B, 2004. **69**.

19. Gu, J.J., et al., *Anisotropy of mobility ratio between electron and hole along different orientations in $\mathrm{Re}{\mathrm{Ge}}_{x}{\mathrm{Si}}_{1.75\ensuremath{-}x}$ thermoelectric single crystals.* Physical Review B, 2005. **71**(11): p. 113201.

20. Qiu, A., et al., *Electronic structure, bonding character, and thermoelectric properties of semiconducting rhenium silicide with doping.* Physical Review B, 2008. **77**(20): p. 205207.

21. Worldwatch Institute. *Global Oil Market Resumes Growth after Stumble in 2009*. 2011 [cited 2016 25 April]; Available from: http://vitalsigns.worldwatch.org/vs-trend/global-oil-market-resumes-growth-after-stumble-2009.

22. Baglione, M.L. *DEVELOPMENT OF SYSTEM ANALYSIS METHODOLOGIES AND TOOLS FOR MODELING AND OPTIMIZING VEHICLE SYSTEM EFFICIENCY*. 2007; Available from: https://deepblue.lib.umich.edu/bitstream/handle/2027.42/57640/mpapke_?sequence=2.

23. Crook, R.F. *14 Rules for Improving Engine Cooling System Capability in High-Performance Automobiles*. 2010; Available from: http://www.zcar.com/forum/12-90-96-tech-discussion-forum/303194-14-rules-improving-engine-cooling-system-capabilities.html.

24. U.S. Department of Energy. *Combined Heat & Power*. 2008; Available from: http://www.midwestchptap.org/cleanenergy/chp/.

25. European Environment Agency. *Pollutant emissons from power plant in European Union*. 2008; Available from: http://www.eea.europa.eu/data-and-maps/data/data-viewers/greenhouse-gases-viewer.

26. Özden, A., et al., *Thermal Conductivity Suppression in Nanostructured Silicon and Germanium Nanowires.* Journal of Electronic Materials, 2016. **45**(3): p. 1594-1600.

27. Minnich, A.J., et al., *Bulk nanostructured thermoelectric materials: current research and future prospects.* Energy & Environmental Science, 2009. **2**(5): p. 466-479.

28. Marcus Newton, S.W., Asher Gomez, Caleb Estherby, *Meta-study: Analysis of thermoelectric figure of merit parameters for silicides with various doping agents.* Students journal, 2016. **3**.

29. Center, N.R. *Electrical Conductivity and Resistivity*. Available from: https://www.nde-ed.org/EducationResources/CommunityCollege/Materials/Physical_Chemical/Electrical.htm.

30. Zhang, X. and L.-D. Zhao, *Thermoelectric materials: Energy conversion between heat and electricity.* Journal of Materiomics, 2015. **1**(2): p. 92-105.

31. Harman, T.C., et al., *Nanostructured thermoelectric materials.* Journal of Electronic Materials. **34**(5): p. L19-L22.

32. Goldsmid, H.J., A.R. Sheard, and D.A. Wright, *The performance of bismuth telluride thermojunctions.* British Journal of Applied Physics, 1958. **9**(9): p. 365.

33. Goldsmid, H.J. and R.W. Douglas, *The use of semiconductors in thermoelectric refrigeration.* British Journal of Applied Physics, 1954. **5**(11): p. 386.

34. Caillat, T., J.P. Fleurial, and A. Borshchevsky, *Preparation and thermoelectric properties of semiconducting Zn4Sb3.* Journal of Physics and Chemistry of Solids, 1997. **58**(7): p. 1119-1125.

35. Venkatasubramanian, R., et al., *Thin-film thermoelectric devices with high room-temperature figures of merit.* Nature, 2001. **413**(6856): p. 597-602.

36. Hsu, K.F., et al., *Cubic AgPbmSbTe2+m: Bulk Thermoelectric Materials with High Figure of Merit.* Science, 2004. **303**(5659): p. 818-821.

37. Heremans, J.P., et al., *Enhancement of Thermoelectric Efficiency in PbTe by Distortion of the Electronic Density of States.* Science, 2008. **321**(5888): p. 554-557.

38. Poudel, B., et al., *High-Thermoelectric Performance of Nanostructured Bismuth Antimony Telluride Bulk Alloys.* Science, 2008. **320**(5876): p. 634-638.

39. Boukai, A.I., et al., *Silicon nanowires as efficient thermoelectric materials.* Nature, 2008. **451**(7175): p. 168-171.

40. Okamura, C., T. Ueda, and K. Hasezaki, *Preparation of Single-Phase ZnSb Thermoelectric Materials Using a Mechanical Grinding Process.* MATERIALS TRANSACTIONS, 2010. **51**(5): p. 860-862.

41. Yang, C.C. and S. Li, *Basic Principles for Rational Design of High-Performance Nanostructured Silicon-Based Thermoelectric Materials.* ChemPhysChem, 2011. **12**(18): p. 3614-3618.

42. Bathula, S., et al., *Enhanced thermoelectric figure-of-merit in spark plasma sintered nanostructured n-type SiGe alloys.* Applied Physics Letters, 2012. **101**(21): p. 213902.

43. Pei, Y., et al., *Convergence of electronic bands for high performance bulk thermoelectrics.* Nature, 2011. **473**(7345): p. 66-69.

44. Shi, X., et al., *Multiple-Filled Skutterudites: High Thermoelectric Figure of Merit through Separately Optimizing Electrical and Thermal Transports.* Journal of the American Chemical Society, 2011. **133**(20): p. 7837-7846.

45. Liu, H., et al., *Ultrahigh Thermoelectric Performance by Electron and Phonon Critical Scattering in Cu2Se1-xIx.* Advanced Materials, 2013. **25**(45): p. 6607-6612.

46. Zhao, L.-D., et al., *Ultralow thermal conductivity and high thermoelectric figure of merit in SnSe crystals.* Nature, 2014. **508**(7496): p. 373-377.

47. He, Y., et al., *High Thermoelectric Performance in Non-Toxic Earth-Abundant Copper Sulfide.* Advanced Materials, 2014. **26**(23): p. 3974-3978.

48. Hicks, L.D. and M.S. Dresselhaus, *Effect of quantum-well structures on the thermoelectric figure of merit.* Physical Review B, 1993. **47**(19): p. 12727-12731.

49. Chen, Z.-G., et al., *Nanostructured thermoelectric materials: Current research and future challenge.* Progress in Natural Science: Materials International, 2012. **22**(6): p. 535-549.

50. Biswas, K., et al., *High-performance bulk thermoelectrics with all-scale hierarchical architectures.* Nature, 2012. **489**(7416): p. 414-418.

51. Kunihito, K., et al., *Oxide Thermoelectric Materials: A Nanostructuring Approach.* Annual Review of Materials Research, 2010. **40**(1 %R doi:10.1146/annurev-matsci-070909-104521): p. 363-394.

52. Bahk, J.-H., et al., *Flexible thermoelectric materials and device optimization for wearable energy harvesting.* Journal of Materials Chemistry C, 2015. **3**(40): p. 10362-10374.

53. Bubnova, O. and X. Crispin, *Towards polymer-based organic thermoelectric generators.* Energy & Environmental Science, 2012. **5**(11): p. 9345-9362.

54. Kim, G.H., et al., *Engineered doping of organic semiconductors for enhanced thermoelectric efficiency.* Nat Mater, 2013. **12**(8): p. 719-723.

55. Zhang, Q., et al., *Organic Thermoelectric Materials: Emerging Green Energy Materials Converting Heat to Electricity Directly and Efficiently.* Advanced Materials, 2014. **26**(40): p. 6829-6851.

56. Mingo, N., et al., *"Nanoparticle-in-Alloy" Approach to Efficient Thermoelectrics: Silicides in SiGe.* Nano Letters, 2009. **9**(2): p. 711-715.

57. Satyala, N. and D. Vashaee, *Modeling of Thermoelectric Properties of MagnesiumSilicide (Mg2Si).* Journal of Electronic Materials, 2012. **41**(6): p. 1785-1791.

58. Auparay, N., *Room Temperature Seebeck Coefficient Measurement*

of Metals and Semiconductors. 2013, Oregon State University. p. 23.

59. Zheng, J.-c., *Recent advances on thermoelectric materials.* Frontiers of Physics in China, 2008. **3**(3): p. 269-279.

60. University of Tennessee, D.o.M.S.a.E., *Electrical Properties*.

61. Han, C., Z. Li, and S. Dou, *Recent progress in thermoelectric materials.* Chinese Science Bulletin, 2014. **59**(18): p. 2073-2091.

62. Physics Handbook, *Wiedemann-Franz Law*.

63. Heng Wang, A.C., Ken Kurosaki, Shinsuke Yamanaka, and G. Jeffrey Snyder, *Reduction of thermal conductivity in PbTe:Tl by alloying with TlSbTe2.* PHYSICAL REVIEW 2011. **B 83**(024303).

64. Tan, G., et al., *Codoping in SnTe: Enhancement of Thermoelectric Performance through Synergy of Resonance Levels and Band Convergence.* Journal of the American Chemical Society, 2015. **137**(15): p. 5100-5112.

65. Lenntech BV. *Periodic table*. Available from: http://www.lenntech.com/periodic/periodic-chart.htm.

66. Bux, S.K., et al., *Mechanochemical synthesis and thermoelectric properties of high quality magnesium silicide.* Journal of Materials Chemistry, 2011. **21**(33): p. 12259-12266.

67. Neophytou, N., *Prospects of low-dimensional and nanostructured silicon-based thermoelectric materials: findings from theory and simulation.* The European Physical Journal B, 2015. **88**(4): p. 1-12.

68. Lee, J.-H. and J.C. Grossman, *Thermoelectric properties of nanoporous Ge.* Applied Physics Letters, 2009. **95**(1): p. 013106.

69. Hochbaum, A.I., et al., *Enhanced thermoelectric performance of rough silicon nanowires.* Nature, 2008. **451**(7175): p. 163-167.

70. Bux, S.K., et al., *Nanostructured Bulk Silicon as an Effective Thermoelectric Material.* Advanced Functional Materials, 2009. **19**(15): p. 2445-2452.

71. Yang, M.-J., Q. Shen, and L.-M. Zhang, *Effect of nanocomposite structure on the thermoelectric properties of 0.7-at% Bi-doped Mg 2 Si nanocomposite.* Chinese Physics B, 2011. **20**(10): p. 106202.

72. Nielsch, K., et al., *Thermoelectric Nanostructures: From Physical Model Systems towards Nanograined Composites.* Advanced Energy Materials, 2011. **1**(5): p. 713-731.

73. *Semiconducting Silicides: Basics, Formation, Properties*, ed. V. Borisenko. 2000: Springer.

74. Hiroki, N., et al., *Effects of Ge substitution on thermoelectric properties of CrSi 2.* Japanese Journal of Applied Physics, 2016. **55**(11): p. 111801.

75. Filonov, A.B., et al., *Semiconducting Properties of Hexagonal Chromium, Molybdenum, and Tungsten Disilicides.* physica status solidi (b), 1994. **186**(1): p. 209-215.

76. Poutcharovsky, D.J. and E. Parthe, *The orthorhombic crystal structure of Ru2Si3, Ru2Ge3, Os2Si3 and Os2Ge3.* Acta Crystallographica Section B, 1974. **30**(11): p. 2692-2696.

77. Mikhail, I.F. and N.I. Grigory, *Silicides: Materials for thermoelectric energy conversion.* Japanese Journal of Applied Physics, 2015. **54**(7S2): p. 07JA05.

78. Wunderlich, W., et al., *Thermoelectric Properties of Mg2Si Produced by New Chemical Route and SPS.* Inorganics, 2014. **2**(2): p. 351.

79. Yang, M., L. Zhang, and Q. Shen, *Synthesis and sintering of Mg2Si thermoelectric generator by spark plasma sintering.* Journal of Wuhan University of Technology-Mater. Sci. Ed., 2008. **23**(6): p. 870-873.

80. Zheng, L., et al., *Optimized nanostructure and thermoelectric performances of Mg2(Si0.4Sn0.6)Sbx solid solutions by in situ nanophase generation.* Journal of Alloys and Compounds, 2016. **671**: p. 452-457.

81. Morris, R.G., *Semiconducting Properties of Mg2Si Single Crystals*. 1957: Iowa State College.

82. M J Yang, L.M.Z., L Q han, Q Shen, and C B Wang, *Simple fabrication of Mg2Si thermoelectric generator by spark plasma sintering.* Indian Journal of Engineering, 2009. **16**: p. 227-280.

83. Jun-ichi, T. and K. Hiroyasu, *Thermoelectric Properties of P-doped Mg 2 Si Semiconductors.* Japanese Journal of Applied Physics, 2007. **46**(6R): p. 3309.

84. Tani, J.-i. and H. Kido, *Thermoelectric properties of Sb-doped Mg2Si semiconductors.* Intermetallics, 2007. **15**(9): p. 1202-1207.

85. Sakamoto, T., et al., *Thermoelectric Characteristics of a Commercialized Mg2Si Source Doped with Al, Bi, Ag, and Cu.* Journal of Electronic Materials, 2010. **39**(9): p. 1708-1713.

86. Isoda, Y., et al., *Thermoelectric Properties of p-Type Mg2.00Si0.25Sn0.75 with Li and Ag Double Doping.* Journal of Electronic Materials, 2010. **39**(9): p. 1531-1535.

87. Isoda, Y., et al., *Effects of Al/Sb Double Doping on the Thermoelectric Properties of Mg2Si0.75Sn0.25.* Journal of Electronic Materials, 2014. **43**(6): p. 2053-2058.

88. Zaitsev, V.K., et al., *Highly effective Mg2Si1-xSnx thermoelectrics.* Physical Review B, 2006. **74**(4).

89. Zhang, Q., et al., *In situ synthesis and thermoelectric properties of La-doped Mg 2 (Si, Sn) composites.* Journal of Physics D: Applied Physics, 2008. **41**(18): p. 185103.

90. Lee, S.-M., D.G. Cahill, and R. Venkatasubramanian, *Thermal conductivity of Si–Ge superlattices.* Applied Physics Letters, 1997. **70**(22): p. 2957-2959.

91. Vining, C.B., et al., *Thermoelectric properties of pressure-sintered Si0.8Ge 0.2 thermoelectric alloys.* Journal of Applied Physics, 1991. **69**(8): p. 4333-4340.

92. Lan, Y., et al., *Enhancement of Thermoelectric Figure-of-Merit by a Bulk Nanostructuring Approach.* Advanced Functional Materials, 2010. **20**(3): p. 357-376.

93. Dismukes, J.P., et al., *Thermal and Electrical Properties of Heavily Doped Ge-Si Alloys up to 1300°K.* Journal of Applied Physics, 1964. **35**(10): p. 2899-2907.

94. Zhu, G.H., et al., *Increased Phonon Scattering by Nanograins and Point Defects in Nanostructured Silicon with a Low Concentration of Germanium.* Physical Review Letters, 2009. **102**(19): p. 196803.

95. Yu, B., et al., *Enhancement of Thermoelectric Properties by Modulation-Doping in Silicon Germanium Alloy Nanocomposites.* Nano Letters, 2012. **12**(4): p. 2077-2082.

96. Lee, E.K., et al., *Large Thermoelectric Figure-of-Merits from SiGe Nanowires by Simultaneously Measuring Electrical and Thermal Transport Properties.* Nano Letters, 2012. **12**(6): p. 2918-2923.

97. Yi, S.-i. and C. Yu, *Modeling of thermoelectric properties of SiGe alloy nanowires and estimation of the best design parameters for high figure-of-merits.* Journal of Applied Physics, 2015. **117**(3): p. 035105.

98. Hou, Q.R., et al., *Thermoelectric properties of higher manganese silicide films with addition of carbon.* physica status solidi (a), 2006. **203**(10): p. 2468-2477.

99. Kikuchi, Y.M.a.Y., ed. *Thermoelectric Nanomaterials*. Higher Manganese Silicide, MnSiγ. Vol. 182. 2013, Springer Series: Japan.

100. Tae-Ho, A., et al., *The Effect of Microstructure on the Thermoelectric Properties of Polycrystalline Higher Manganese Silicides.* Japanese Journal of Applied Physics, 2013. **52**(10S): p. 10MC11.

101. Truong, D.Y.N., *Thermoelectric Properties of Higher Manganese Silicides*, in *Doctor of Philosophy in Chemistry* 2015, University of Waterloo: Canada. p. 189.

102. Girard, S.N., et al., *Thermoelectric Properties of Undoped High Purity Higher Manganese Silicides Grown by Chemical Vapor Transport.* Chemistry of Materials, 2014. **26**(17): p. 5097-5104.

103. Itoh, T. and M. Yamada, *Synthesis of Thermoelectric Manganese Silicide by Mechanical Alloying and Pulse Discharge Sintering.* Journal of Electronic Materials, 2009. **38**(7): p. 925-929.

104. Ikuto, A., et al., *Doping Effects on Thermoelectric Properties of Higher Manganese Silicides (HMSs, MnSi 1.74) and Characterization of Thermoelectric Generating Module using p -Type (Al, Ge and Mo)-doped HMSs and n -Type Mg 2 Si 0.4 Sn 0.6 Legs.* Japanese Journal of Applied Physics, 2005. **44**(6R): p. 4275.

105.   Luo, W., et al., *Improved Thermoelectric Properties of Al-Doped Higher Manganese Silicide Prepared by a Rapid Solidification Method.* Journal of Electronic Materials, 2011. **40**(5): p. 1233-1237.

106.   Ikuto, A., et al., *Effects of Ge Doping on Micromorphology of MnSi in MnSi ~1.7 and on Their Thermoelectric Transport Properties.* Japanese Journal of Applied Physics, 2005. **44**(12R): p. 8562.

107.   Koyama, T., et al., *Crystal Structure and Thermoelectric Properties of Mn-Substituted Ru2Si3 with the Chimney-Ladder Structure.* MRS Online Proceedings Library Archive, 2008. **1128**: p. 1128-U05-01 (6 pages).

108.   Norouzzadeh, P., et al., *The effect of nanostructuring on thermoelectric transport properties of p-type higher manganese silicide MnSi1.73.* Journal of Applied Physics, 2012. **112**(12): p. 124308.

109.   Ur, S.-C., I.-H. Kim, and J.-I. Lee, *Properties of Co-doped N-type FeSi2 processed by mechanical alloying.* Metals and Materials International, 2002. **8**(2): p. 169-175.

110.   Ware, R.M. and D.J. McNeill, *Iron disilicide as a thermoelectric generator material.* Electrical Engineers, Proceedings of the Institution of, 1964. **111**(1): p. 178-182.

111.   S. J. Hong, C.K.R., B. S. Chun, *Phase Transition and Thermoelectric Property of Ultra-fine Structured*

β-FeSi2 Compounds. Solid State Phenomena, 2006. **118**: p. 591-596.

112.   Hasaka, T.W.a.M., *Thermoelectric Properties of Iron Silicide Based SemiconductorsFabricated by Dip-Treatment into Silver Nitrate Solution.* J. Japan Inst. Metals, 1999. **63**(4): p. 508-514.

113.   Hasaka, M., et al. *Thermoelectric properties and microstructure of Co-doped iron-silicides mixed with Ag or Cu.* in *ICT 2005. 24th International Conference on Thermoelectrics, 2005.* 2005.

114.   Kim, S.W., et al., *High temperature thermoelectric properties of p- and n-type β-FeSi2 with some dopants.* Intermetallics, 2003. **11**(5): p. 399-405.

115.   Cronin, B.V., *Thermoelectric Properties of Silicides*, in *CRC Handbook of Thermoelectrics*. 1995, CRC Press.

116.   Eupene Belyaev, G.S., Aleksey Ancharov, Stanislav Avramchuk, and S.M. Nikolay Slavnykh, and Oleg Lomovsky, *MECHANOCHEMICAL PRODUCTION AND INVESTIGATION OF*

NANOCOMPOSITE THERMOELECTRIC CERAMICS ON THE BASE

OF HEAVY MULTICOMPONENTS DOPED P-FeSi2 Institute of Solid State Chemistry and Mechanochemistry: Novosibirsk.

117.   Mattheiss, L.F., *Structural effects on the calculated semiconductor gap of* ${\mathrm{CrSi}}_{2}$. Physical Review B, 1991. **43**(2): p. 1863-1866.

118.   Perumal, S., et al., *Thermoelectric properties of chromium disilicide prepared by mechanical alloying.* Journal of Materials Science, 2013. **48**(17): p. 6018-6024.

119.   Pandey, T. and A.K. Singh, *Origin of enhanced thermoelectric properties of doped CrSi2.* RSC Advances, 2014. **4**(7): p. 3482-3486.

120.   Dasgupta, T., et al., *Structural, thermal, and electrical properties of CrSi2.* Journal of Applied Physics, 2008. **103**(11): p. 113516.

121.   S. PERUMAL, S.G., U. AIL, R. DECOURT, and a.A.M. UMARJI, *Effect of Composition on Thermoelectric Properties*

of Polycrystalline CrSi2. Journal of ELECTRONIC MATERIALS, 2013. **42**(6).

122.   Perumal, S., et al., *Effect of co-substitution of Mn and Al on thermoelectric properties of chromium disilicide.* Journal of Materials Science, 2013. **48**(1): p. 227-231.

123.   Kajikawa, T., et al. *Thermoelectric properties of high temperature transition metal silicides prepared by spark plasma sintering method*. in *Thermoelectrics, 1999. Eighteenth International Conference on*. 1999.

124.   Dasgupta, T. and A.M. Umarji, *Role of milling parameters and impurity on the thermoelectric properties of mechanically alloyed chromium silicide.* Journal of Alloys and Compounds, 2008. **461**(1–2): p. 292-297.

125.   Hsu, H.-F., P.-C. Tsai, and K.-C. Lu, *Single-crystalline chromium silicide nanowires and their physical properties.* Nanoscale Research Letters, 2015. **10**(1): p. 1-8.

126.   Zhou, F., et al., *Determination of Transport Properties in Chromium Disilicide Nanowires via Combined Thermoelectric and Structural Characterizations.* Nano Letters, 2007. **7**(6): p. 1649-1654.

127.   Krivosheev, A.E., et al., *Thermoelectric efficiency of single crystal semiconducting ruthenium silicide.* Semiconductors, 2006. **40**(1): p. 27-32.

128.   Fedorov M.I., I.Y.V., Vedernikov M.V., Zaitsev V.K, *Iron disilicide as a base for new*

improved thermoelectrics creation // Material Research Society Symposium Proceedings. 1999. **545**: p. 155-160.

129.   Poutcharovsky D.J., Y.K., Parthe´ E, *Diffusionless phase transformations of Ru2Si3, Ru2Ge3 and Ru2Sn3 I. Crystal structure investigations.* 1975. **40**: p. 139-144.

130.   Souptel, D., et al., *Floating zone growth and characterization of semiconducting Ru2Si3 single crystals.* Journal of Crystal Growth, 2002. **244**(3–4): p. 296-304.

131. Vining, C.B., *Space nuclear power station*, in *AIP conference*, M.S.E.-G.a.M.D. Hoover, Editor. 1992, American Institue of Physics.

132. Allevato, C.B.V.a.C.E., *Progress in Doping of Ruthenium Silicide (Ru2Si3).* 1992: p. 3489-3492.

133. Ivanenko, L.I., et al., *Electronic properties of semiconducting silicides: fundamentals and recent predictions.* Thin Solid Films, 2004. **461**(1): p. 141-147.

134. Longhin, M., et al., *Nanostructured CoSi Obtained by Spark Plasma Sintering.* Journal of Electronic Materials, 2015. **44**(6): p. 1963-1966.

135. Hsu, C.C., et al., *Effect of local atomic and electronic structures on thermoelectric properties of chemically substituted CoSi.* EPL (Europhysics Letters), 2014. **106**(3): p. 37007.

136. He, G., et al., *Preparation and electrochemical hydrogen storage property of alloy CoSi.* Electrochemistry Communications, 2006. **8**(10): p. 1633-1638.

137. Z. J. Pan, L.T.Z., and J. S. Wu, *Electronic structure and transport properties of doped CoSi single crystal.* JOURNAL OF APPLIED PHYSICS, 2007. **101**: p. 033715.

138. T. A. Nguyen Tan, J.Y.V., P. Muret, S. Kennou, A.Siokou, S. Ladas, F. L. Razafindramisa, and M. Brunel, Appl. Phys, 1995. **77**: p. 2514.

139. Sakamaki Y., K.K., Jiajun G., Inui H., Yamaguchi M., Yamamoto A., Obara H, *Crystal structure and thermoelectric properties of ReSi1.75 based silicides.* Materials Science Forum, 2003. **426-432**: p. 1777-1782.

140. Inui, H., *Rhenium silicide as a new class of thermoelectric material.* MRS Proceedings, 2005. **886**.

141. Filonov, A.B., et al., *The transport and thermoelectric properties of semiconducting rhenium silicide.* Semiconductors, 2005. **39**(4): p. 395-399.

Chapter 6: Appendices

Nomenclature

ZT	Dimensionless figure of merit
σ	Electrical conductivity
S	Seebeck coefficient
k	Thermal conductivity
k_l	Lattice thermal conductivity
k_e	Electric thermal conductivity
ρ	electrical resistivity
T	absolute temperature
n	carrier concentration
μ	carrier mobility
e	unit of charge carrier
T_c	cold side temperature
T_H	Hot side temperature
η_H	efficiency of power generation
η_C	efficiency of cooling system
L	Lorentz number
V	Thermoelectric voltage